Experimental and Theoretical Studies on Ants Foraging

Sakiyama, Tomoko

(Degree)
博士（理学）

(Date of Degree)
2015-03-25

(Date of Publication)
2017-03-25

(Resource Type)
doctoral thesis

(Report Number)
甲第6335号

(URL)
https://hdl.handle.net/20.500.14094/D1006335

Doctoral Dissertation

博士論文

Experimental and Theoretical Studies on Ants Foraging

（アリの探索行動に関する実験および理論的研究）

January 2015

Graduate School of Science

Kobe University

Tomoko Sakiyama

崎山朋子

CONTENTS

Chapter 1: Introduction **1**

Chapter 2: Random Walk Models:
Emergence of Power-Law Movements **5**

2-1 Emergence of optimal searching from Brownian walks
- 2-1-1 BACKGROUND 6
- 2-1-2 MATERIALS & METHODS 8
- 2-1-3 RESULTS 10
- 2-1-4 DISCUSSION 14

2-2 The relationship between "randomness" and "power-law" on Lévy-like foraging
- 2-2-1 BACKGROUND 16
- 2-2-2 MATERIALS & METHODS 17
- 2-2-3 RESULTS 20
- 2-2-4 DISCUSSION 23

2-3 Weber-Fechner relation derived from interactions in random walk strategy
- 2-3-1 BACKGROUND 26
- 2-3-2 MATERIALS & METHODS 27
- 2-3-3 RESULTS 30
- 2-3-4 DISCUSSION 34

2-4 Lévy-like movements in Japanese carpenter ants
- 2-4-1 BACKGROUND 37
- 2-4-2 MATERIALS & METHODS 38
- 2-4-3 RESULTS 41
- 2-4-4 DISCUSSION 46

Chapter 3: Logical Foraging and Visual Navigation in Foraging Ants **47**

3-1 Visual learning and foraging in Japanese carpenter ants
- 3-1-1 BACKGROUND 48
- 3-1-2 MATERIALS & METHODS 48
- 3-1-3 RESULTS 51
- 3-1-4 DISCUSSION 53

Chapter 4: Kanizsa Triangle Illusion:
Weak Cognition **55**

4-1 Human perception formed and destroyed by local obstacles or foraging ants
- 4-1-1 BACKGROUND 56
- 4-1-2 MATERIALS & METHODS (Human experiments) 57
- 4-1-3 RESULTS (Human experiments) 60
- 4-1-4 MATERIALS & METHODS (Ant experiments) 64
- 4-1-5 RESULTS (Ant experiments) 65
- 4-1-6 DISCUSSION 66

Appendix **68**

Chapter 1

Introduction

1 Introduction

Living systems, including human, show sometimes unpredictable behavior. We mainly focus on ant's foraging navigation such as visual landmarks or random foragers' movements, in which unpredictable phenomenon emerges. It is well known that these amazing behaviors play an important role for agents to maintain current situation on one hand, and adjust to unknown environments on the other hand. These behaviors are generally called flexible behaviors. In many researches, inserting external noises induce agents to realize those movements. However, inside or outside is completely distinguished from the other in these models. Sometimes their movements are deviated by noises, though. Agents only have to obey their own experienced memories or determined rules. Therefore, simple errors may be key points by tuning the parameters from outside, i.e. by experimenters in these models.

How can we explain those animals' behaviors without assuming any transcendent observations? Those movements would be naturally obtained by loosely connecting distinguished outside with inside, resulting in attaining a new behavior and at the same time persisting recurrent movements for agents. Agents might refer to global property and concurrently hold ambiguity with using local information, which contributes to achieve mentioned scenario.

In this paper, we describe three main topics with respect to ants' foraging navigations or movement. Many ant species are known to form their own colonies. Ant foragers and colonies are well-often studied to investigate self-organized systems or adaptive modelling in order to solve complex cognitive tasks. Although there is no leader in ant colonies, they can show optimal strategies in order to survive. Here we examined whether or not their adaptive/optimal behaviors were achieved by confusing different level in mechanisms or materials.

One is agent-based random walk simulation models (chapter 2). It is well discussed whether animals' movements follow Lèvy walk or not. Lèvy foragers make step lengths on each time which have probability density distribution with power-law tail. Therefore, these foragers exhibit supper-diffusion property which is not observed in Brownian walkers. Many researchers have tackled on whether animals show Lèvy walk or not. However, it seems that it is difficult to strictly judge the properties of their movements, because animals show different movement properties depending on surrounding contexts. Here, we developed two different models to explain the origin of Lèvy walk in chapter 2.

The first one is a single-agent random walk model in which an agent changes its directional rules in order to maintain unbiased movements. In our algorithm, the agent's memory ability is restricted. Therefore, the agent can pursue only recent limited trajectories. Thus, the agent produces wrong interpretations regarding to biased movements, resulting in emergence of more biased

movements. We succeeded in inducing the agent to show power-law movements.

Regarding to ants movement strategy, desert ants are known to show Brownian motion when they forage individually. However, as already mentioned, it is plenty room to investigate whether they show Lèvy walk or not when they swarm or interact with other agents. Therefore, we conducted foragers' movement experiments using Japanese carpenter ants and obtained they showed Lèvy-like movements when they swarmed. We also conducted multi-agent model in which each agent interacted with each other by locally predicting other's moving direction and changed directional rules with active deviations. Our results fitted to those of experimental analysis.

For agents, in both algorithms, odd behaviors are induced thanks to referring to global properties based on local information and at the same time holding ambiguities due to their limited abilities. These ambiguities could be key roles to achieve flexible movements.

Second, we conducted visual navigation experiments using Japanese carpenter ants (chapter 3). Ant foragers use several navigation systems to locate profitable food locations or their nests. Recruitments using chemical pheromones are well known. In addition to that, foragers also use visual stimulus for their navigation. There are numerical studies to investigate how visual landmarks, panoramic views or celestial compasses are used for their orientations. Ant foragers do not appear to use cognitive maps (locale systems). Rather, they depend on taxon-like systems in which one-to-one correspondences between agents' current position and next moving-direction are implemented. Thus, the matched direction is always the direction in which to travel. However, this inability does not exclude the possibility that ants cannot use map-like navigation. The idea of each navigate-system (locale or taxon) is an extreme case in navigation; thus, in identifying the role of the map, we assume that ants can identify a pair of visual and accessible cues (accessibility) from a common stimulus.

We here demonstrate that ants can use a local cognitive map in which logical operations with respect to accessibility are employed in navigation. We introduced several distinguishable visual stimuli for ant foragers. These stimuli leaded to several food locations or dead-ends. We could obtain that foragers could learn a set of accessible cues using logical operations (AND or XOR). More interestingly, foragers appeared to produce new symbols or landmarks to get rid of the inconsistences aroused from logical operations. Therefore, from interrnal noises, ants sometimes appear to directly go to unknown landmarks or panoramic directions, resulting in achievement of find new food locations during their homing trips.

Finally, we examined whether ants show Kanizsa-triangle illusion or not (chapter 4). Kanizsa triangle figure, in which three Pac-Man-shaped figures are turned inside symmetrically, is well known as an illusion figure. Subjective contour is perceived although such contour actually never exists. Regarding to perceptions, it is well discussed whether animals, including human, perceive the whole pictures or just element part level. However, in any case, it seems that there is a

tendency to make judgment which level is true or not, in assuming that each level is independent of each other. Some studies reported that experimental subjects' persistency to either level is changeable depending on situation contexts. Therefore, there is plenty of space to investigate new mechanism in order to explain above flexible decision making, i.e. employing local element information while concurrently referring to global properties. As already mentioned, ants appear to flexibly use local information. Therefore, tracking foragers' trajectories by exposing them to Kanizsa-shaped solution food might be compared with an abstract model in which global properties (Kanizsa-triangle illusion) were produced based on bottom-up processes. When ants were exposed to Kanizsa-triangle shaped figures, triangle trajectories along each Pac-man's mouths were obtained in our experiments. We also conducted cognitive experiments using human subjects in which obstructive stripe notches were equipped to each Pac-man to investigate whether or not subjects' whole perceptions were affected by these notches. Illusion contour appeared to depend on the location and direction of the stripe notches. Therefore, also in human, local disturbed patterns may contribute to form the dynamic global perceptions.

In summary, agents can achieve optimal searching or foraging when they confuse and identify different level mechanisms or materials such like a pair of others' movement and movement-rule or a pair of visual cues and those meanings. Thanks to those identifications, agents might actively produce wrong and odd interpretations or landmarks. These errors or falsity would play an important role to maintain the balance between persistence of current situations (exploitation) and discovering new items (exploration) without inserting any external noises. Therefore, our researches would contribute to produce autonomous human-like agents which change the parameters by themselves without any coordinating by experimenters.

Chapter 2

Random Walk Models: Emergence of Power-Law Movements

2-1 Emergence of optimal searching from Brownian walks

2-1-1. BACKGROUND

When agents can exploit previously acquired knowledge, such as profitable food locations or the cost required to reach those locations, selecting an effective route entails solving a so-called deterministic walk problem, such as the "travelling tourist problem" [1,2]. On the contrary, in the absence of prior knowledge, "chance" or "randomness" represents a more appropriate scenario for exploring an unknown environment, and many random search algorithms, such as the Lévy walk or the Brownian walk algorithm, are effective for random exploration and have been very well studied [3-7].

The Lévy walk is defined as a process whereby an agent takes steps of length l at each time, and l shows a probability density distribution with a power-law tail:

$$P(l) \sim l^{\mu}$$

where $1<\mu \leqq 3$. A Lévy walk with $\mu \approx 2$ results in optimal random searches in environments with randomly distributed food sites [8]. For $\mu>3$, the Lévy walk converges to Brownian motion. In environments with extremely abundant resources, the Lévy and Brownian walk food-searching algorithms result in similar exploration efficiencies. However, the Lévy walk is more suitable than the Brownian walk for searching in low-density environments, and Lévy foragers can survive for longer periods of time without extinction [9,10].

To determine which algorithm is more suitable for modeling animal movement behavior, recent analyses have made comparisons between an animal's actual movements and model simulations and have attempted to determine whether the movements correspond to a Lévy walk [8,11] or to a Brownian walk [12]. However, it appears that, in searching for food, animals do not depend on a particular type of movement modeled by a certain algorithm, but rather, the rules guiding their movement change depending on the context [13,14].

Therefore, in determining an animal's foraging behavior, its interactions with the environment and/or its effects on the surrounding world, the issue that arises is not only the determination of the optimal algorithm for a random walk but also the estimation of how these flexible behaviors arise from what that animal is doing [15].

When an agent's movement obeys a certain distribution, that agent behaves exclusively according to the probabilistic rule determining the distribution. From this perspective, the direction and step length are completely determined by a roll of the dice, which is independent of whether the dice are biased.

If an agent behaving according to a random movement rule sometimes alters the next step forward or the rule itself, then the resulting movement does not follow the distribution resulting from a random roll of the dice and the application of the abovementioned rule. Thus, a balancing of chance with necessity or of a passive with an active movement mode must be achieved by the agent's interaction with its surroundings.

Here, starting with a simple random walk with uniform step length and discrete angle distributions, we consider an agent who alters the rule that controls him based on his own experiences, and we propose an effective exploration algorithm (REV, a random walk algorithm) despite the fixed step lengths. In this study, the agent experiences random directional biases; based on these biases, he disregards the rule that he had been obeying until that time and changes the rule itself using his memory, which was obtained by chance, to implement an indeterminate forward step that is independent of the rule. There are few studies detailing agent movements for agents who proceed with unknown forward steps based on limited memories of their own experiences [16]. We also report the emergence of a power-law distribution that is independent of step length.

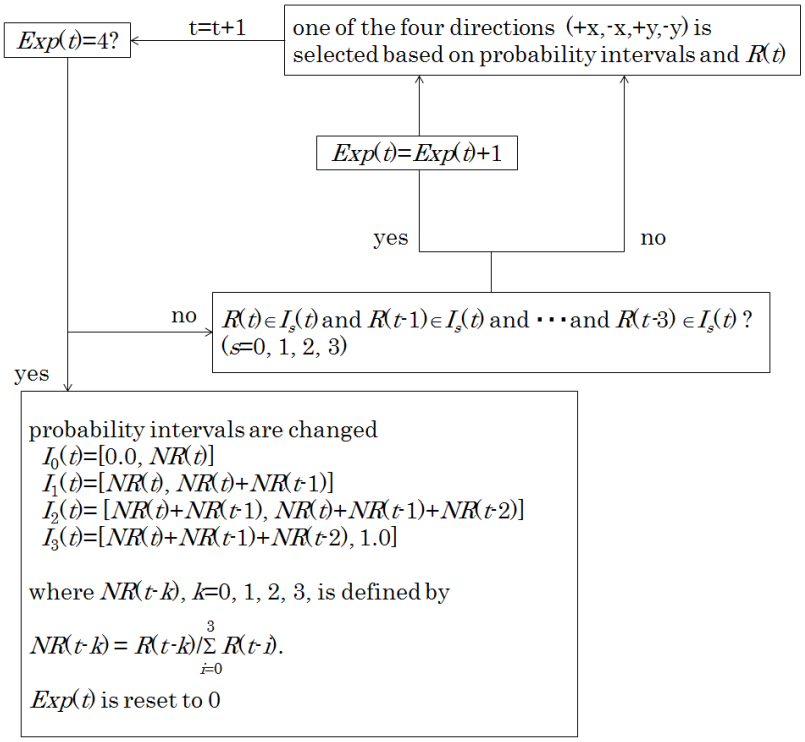

Figure 1. Flow chart of the REV-Random algorithm. In each trial, the probability intervals $I_s(t)$ (s=0, 1, 2, 3) were initially set to $I_0(0)$=[0.0, 0.25], $I_1(0)$=[0.25, 0.5], $I_2(0)$=[0.5, 0.75] and $I_3(0)$=[0.75, 1.0] until these intervals were changed. Therefore, each trial started with a simple random walk. $R(t)$ indicates the random number at the tth step. $Exp(t)$ indicates the experience number for directional moves, that is, the number of consecutive moves in the same direction, such as $+x$, $+x$, $+x$, $+x$. See

also the above text.

2-1-2. MATERIALS & METHODS

(a) *2D simple random walk*

Each trial is run for a maximum of 10,000 time steps. First, we use a simple two-dimensional (2D) random walk to set the simulation stage for each trial and set the agent at the origin. In this algorithm, a random number from 0.00 to 1.00 is selected at each time step. We assume that the agent moves in two-dimensional square lattices. The agent selects one direction among four discrete directions, +x, -x, +y or -y, depending on a random number classified to one of the following four intervals, [0.0, 0.25], [0.25, 0.5], [0.5, 0.75] or [0.75, 1.0]. For example, if the random number is 0.23 at the tth step (i.e., R(t)=0.23), the agent steps forward +1 along the x axis. We create an agent that, depending on its experiences, alters the rule that controls that agent's movement directions.

(b) *2D REV-random walk (REV-Random)*

In our Re-valued (REV) random walk model, at the tth step, the agent has a memory that gives it access to four random numbers, from $R(t)$ to $R(t\text{-}3)$. This model implies that the agent has a limited memory. While the agent in the simple random walk has access to only one random number, $R(t)$, and the interval controlling the agent's move is fixed, the interval in the REV random walk, $I_s(t)$, s=0, 1, 2, 3, is changed using the four random numbers when the succession of the agent's directional moves exceeds a threshold number. The four intervals are initially set to $I_0(0)$=[0.0, 0.25], $I_1(0)$=[0.25, 0.5], $I_2(0)$=[0.5, 0.75] and $I_3(0)$=[0.75, 1.0]. The next walk is defined by the following equations:

$$(x(t+1), y(t+1)) = (x(t)+1, y(t)), \text{ if } R(t)\in I_0(t); \quad =(x(t)-1, y(t)), \text{ if } R(t)\in I_1(t);$$
$$=(x(t), y(t)+1), \text{ if } R(t)\in I_2(t); \quad =(x(t), y(t)-1), \text{ if } R(t)\in I_3(t),$$

Thus, every trial starts as a simple random walk.

A directional move that consists of a series of the same move, such as $+x, +x, +x, \ldots$ is counted as follows:

$$Exp(t+1)=Exp(t)+1, \quad \text{if } R(t)\in I_s(t), R(t\text{-}1)\in I_s(t), R(t\text{-}2)\in I_s(t), R(t\text{-}3)\in I_s(t)$$
$$\text{for some } s \text{ in } \{0, 1, 2, 3\};$$
$$Exp(t+1)=Exp(t), \quad \text{otherwise.}$$

For example, if the agent's directional move from t-3 to t corresponds to a $+y$, $+y$, $+y$, $+y$ series, it implies

$$R(t)\in I_2(t), R(t\text{-}1)\in I_2(t), R(t\text{-}2)\in I_2(t), R(t\text{-}3)\in I_2(t)$$

Therefore

$Exp(t+1)=Exp(t)+1$

However, if the agent's directional move from t-3 to t corresponds to $+y$, $+x$, $+y$, $+y$, then it implies

$R(t)\in I_2(t)$, $R(t\text{-}1)\in I_0(t)$, $R(t\text{-}2)\in I_2(t)$, $R(t\text{-}3)\in I_2(t)$

Therefore

$Exp(t+1)=Exp(t)$

If $Exp(t)$ exceeds a threshold number, θ, the four intervals are changed as follows:

$$I_0(t)=[0.0, NR(t)], \qquad I_1(t)=[NR(t), NR(t)+NR(t\text{-}1)],$$
$$I_2(t)= [NR(t)+NR(t\text{-}1), NR(t)+NR(t\text{-}1)+NR(t\text{-}2)], \qquad I_3(t)=[NR(t)+NR(t\text{-}1)+NR(t\text{-}2), 1.0],$$

where $NR(t\text{-}k)$, k=0, 1, 2, 3, is defined by

$$NR(t\text{-}k) = R(t\text{-}k)/\sum_{i=0}^{3} R(t\text{-}i).$$

When $Exp(t)$ exceeds θ, $Exp(t)$ is reset to 0.

For example, if $Exp(t)$ exceeds θ and $R(t\text{-}3)$=0.20, $R(t\text{-}2)$=0.15, $R(t\text{-}1)$=0.10 and $R(t\text{-}3)$=0.20, then $NR(t\text{-}k)$ for k=0, 1, 2, 3 is given as follows:

$NR(t\text{-}3)$=0.20/(0.20+0.15+0.10+0.20)=0.31

$NR(t\text{-}2)$=0.15/(0.20+0.15+0.10+0.20)=0.23

$NR(t\text{-}1)$=0.10/(0.20+0.15+0.10+0.20)=0.15

$NR(t)$=0.20/(0.20+0.15+0.10+0.20)=0.31

Thus, $I_s(t)$ for s=0,1,2,3 is given as follows:

$I_0(t)$=[0.0, 0.31]

$I_1(t)$=[0.31, 0.31+0.15]=[0.31, 0.46]

$I_2(t)$=[0.31+0.15, 0.31+0.15+0.23]=[0.46, 0.69]

$I_3(t)$=[0.31+0.15+0.23, 0.31+0.15+0.23+0.31]=[0.69, 1.00]

Finally, $Exp(t)$ is reset to 0.

The flow chart of the REV-random walk algorithm is presented in Figure 1.

In our simulations, θ is set to 4, and we discuss the agent's behavioral differences between θ=4 and θ=8, 64 and 128.

In the simple random walk algorithm, the probability of a random number falling into a particular interval is 0.25, as the intervals are divided equally. Thus, the agent moves north, east, west or south with equal probability. In contrast, the intervals in the REV-random walk algorithm are divided

unequally, depending on the agent's history.

2-1-3. RESULTS

(a) *Threshold θ=4*

Figure 2 shows an example of an agent trajectory for each algorithm. Compared to a simple random walk, the agent can reach farther areas by following the REV-Random algorithm while spending longer amounts of time in certain areas.

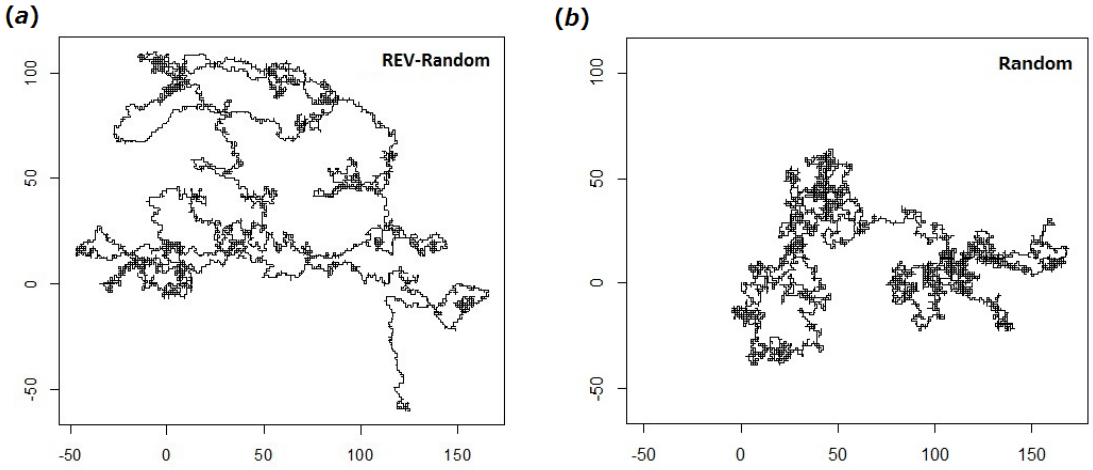

Figure 2. Example of an agent trajectory after 10,000 time steps of each algorithm. (*a*) REV-Random. (*b*) Random.

In the simple random walk analysis, it is known that the mean squared distance and time step are related by the following relation [5,17]:

$$\langle R^2 \rangle \sim t^{2H}$$

Parameter H is determined depending on the algorithm (H>1/2 for a Lévy walk (super-diffusion), H=1/2 for a correlated random walk with more than 10^2 time steps or for a Brownian walk (diffusion)). Figure 3 shows the mean squared distance and the time step obtained from our algorithm (the averaged R^2 was obtained from 1,000 trials at each discrete time step). The fit for parameter H according to the above model was H~0.61, indicating that super-diffusion was achieved (N=19, R-squared=0.99, F=2,109.00, P<1.0e-15). We also checked the degree of diffusion by restricting the fit to the largest five values of the time step because it appeared that H converged to H~1/2. However, we found that the fit was H~0.57 (N=5, R-squared=0.99, F=1,108.00, P<1.0e-4).

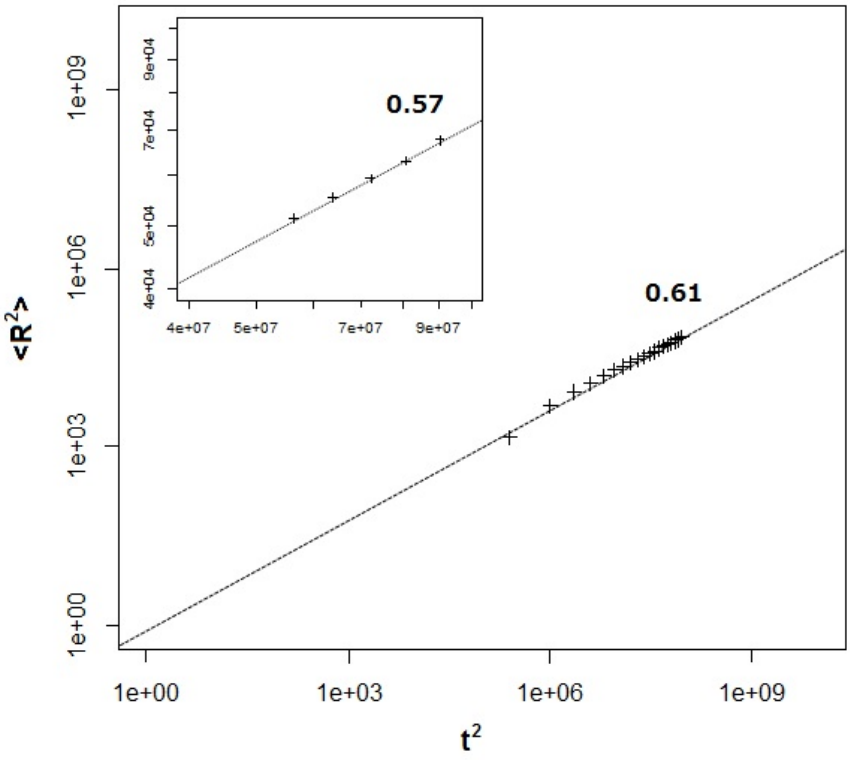

Figure 3. Log-scale plot of $<R^2>$ and t^2. The inset is an expansion of the *x*-axis showing the five largest values (see also the text).

To evaluate the exploration efficiency, we established four feeder sites consisting of 10×10 squares distributed as shown in Figure 4b. The agent is initially set at the center of the foraging region (starting point). If the agent reaches one of the four fixed sites, the time step required to reach the site is the output. We conducted 100 trials based on each algorithm and estimated how frequently the agent could reach an individual feeder in a limited period of 10,000 time steps. Figure 4a presents a comparison of the performance of the REV-Random and simple random walk algorithms. If the feeder sites are closely located, within 10 to 20 distance units from the starting point (Figure 4b), an agent can reach a feeder site in 10,000 steps under both algorithms. However, if the feeder sites are located farther away from the starting point, at 110 to 120 distance units, the performance of the REV-Random algorithm is better than that of the simple random walk algorithm (number of successes in 10,000 steps, REV-Random vs. Random, 10-20: 96 vs. 98, Fisher test, P=0.36, NS; 60-70: 64 vs. 62, chi-squared test, χ^2_2=0.022, P=0.88, NS; 110-120: 32 vs. 13, chi-squared test, χ^2_2=9.29, P<0.001).

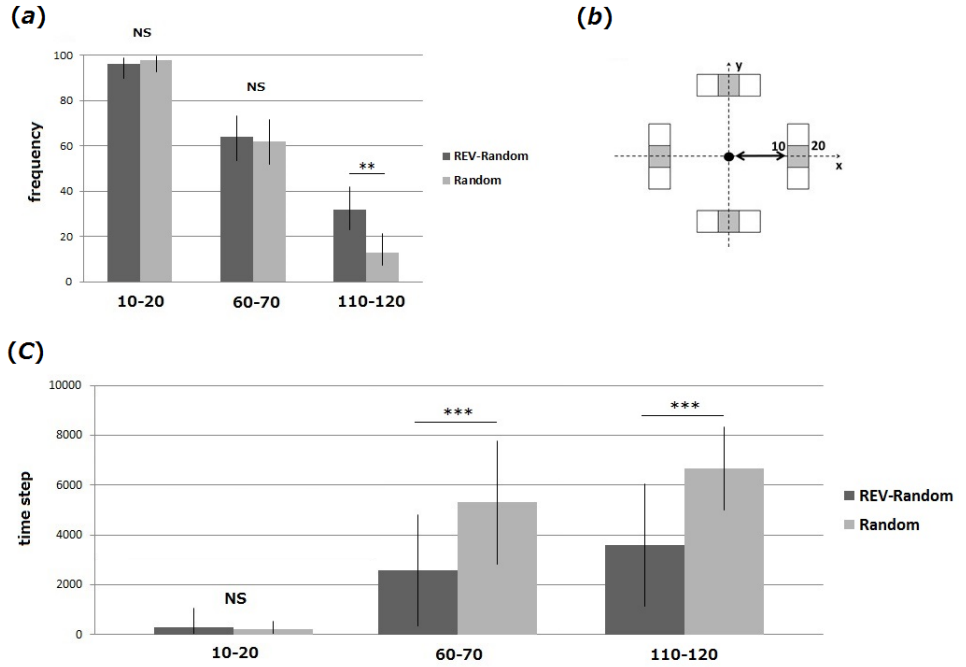

Figure 4. (*a*) Frequency of successfully reaching one of the feeder sites within 10,000 time steps for each algorithm run for 100 trials. (*b*) Example of feeder site locations. Here, the 10-20 version is sketched. The black dot in the center indicates the origin of the coordinates. The four grey zones indicate feeder sites. Each feeder site occupies a 10 ×10 grid size and is fixed on one of the two axes in each direction away from the origin. The notation 10-20 indicates that the distance from the origin to the feeder areas is 10 units. (*c*) Average number of time steps required to reach one of the four feeder sites in each trial for each algorithm run for 100 trials. Straight lines indicate error bars. **P<0.01, ***P<0.001, NS indicates not significant.

We estimated not only whether an agent reaches the target but also the time required to reach the feeder (Figure 4c). There is no significant difference between the two algorithms when the feeder is 10 to 20 distance units away from the center (REV-Random vs. Random, $N_{REV\text{-}R}$=96, N_R=98, $MEAN_{REV\text{-}R}$=303.7±753.2, $MEAN_R$=235.4±302.8, Mann-Whitney U test, U=4,592.0, p=0.69, NS) (Figure 4c). However, in the other cases, the agent following the REV-Random algorithm can reach the feeder site significantly faster than that following the random walk algorithm, even when the feeder is placed at a middle-range distance away from center (REV-Random vs. Random, 60-70: $N_{REV\text{-}R}$=64, N_R=62, $MEAN_{REV\text{-}R}$=2,589.0±2,239.4, $MEAN_R$=5,003.0±2,480.1, Mann-Whitney U test, U=761.00, P<0.001, 110-120: $N_{REV\text{-}R}$=32, N_R=13, $MEAN_{REV\text{-}R}$=3,596.0±2,467.6, $MEAN_R$=6,670.0±1,657.9, Mann-Whitney U test, U=761.00, P<0.001). Thus, the REV-Random algorithm is more efficient at exploring both nearby (but not very close) and distant areas within a certain limited time.

When considering the final location of the agent after 10,000 time steps for 100 trials using each algorithm, we found that there was no relationship between the x and y coordinates for either algorithm (REV-Random, *R*-squared=-0.01, *F*=0.0041, *P*=0.95, NS; Random, *R*-squared=-0.0057, *F*=0.44, *P*=0.51, NS) (Figure S1).

Figure 5 provides a histogram of the time duration (in units of time steps) between rule change events. Interestingly, we found that the histogram shows a power-law distribution. (power-law vs. exponential, N=57, μ=1.85, λ=0.0063, w_p=0.97, w_{exp}=0.03, goodness of fit test: G=41.39, df=36, P=0.25) [18]. We discuss the significance of this finding in the next section..

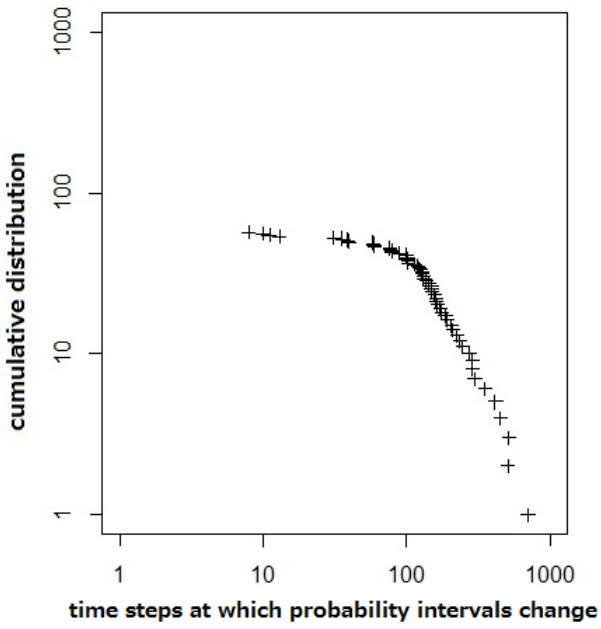

Figure 5. Log-scale plot of the distribution of time intervals between rule change events.

(b) *Difference between θ=4 and other threshold values (8, 64 and 128)*

We further investigated how θ threshold values affect the exploration process. Here, we compare a threshold of 4 with a threshold of 8 using the same analytical process described above (i.e., based on the ability to reach a target within a certain distance or within a certain time limit). According to Figure 6a, the threshold 8 REV-Random algorithm is not as efficient as the threshold 4 version with respect to the exploration efficiency (number of successes in 10,000 steps for threshold 4 vs. threshold 8, 10-20: 96 vs. 92, chi-squared test, χ^2_2=0.80, P=0.37, NS; 60-70: 64 vs. 36, chi-squared test, χ^2_2=14.6, P<0.001; 110-120: 32 vs. 27, chi-squared test, χ^2_2=0.38 P=0.54, NS). We also evaluated the distance between the start and end points after 10,000 steps for four different threshold values (4, 8, 64 and 128). Figure 6b shows that the distance increases depending on the threshold values, suggesting that changing the current rule affects the agent's bias towards movement in a

straight line (threshold 4 vs. threshold 8: N_4=100, N_8=100, $MEAN_4$=246.0±149.5, $MEAN_8$=295.6±174.5, Mann-Whitney U test, U=4122.5, P<0.05; threshold 4 vs. threshold 64: N_4=100, N_{64}=100, $MEAN_4$=246.149.5±149.5, $MEAN_{64}$=526.2±318.5, Mann-Whitney U test, U=2172.0, P<1.0E-11). However, we observed no significant difference between a threshold of 4 and a threshold of 128 (threshold 4 vs. threshold 128: N_4=100, N_{128}=100, $MEAN_4$=246.0±149.5, $MEAN_{128}$=323.4±259.2, Mann-Whitney U test, U=4436.0, P=0.17, NS). As can be seen from Figure S2, the changing of the current rule occurs less often as threshold values increase, and the areas with a concentrated presence become larger until the first rule change.

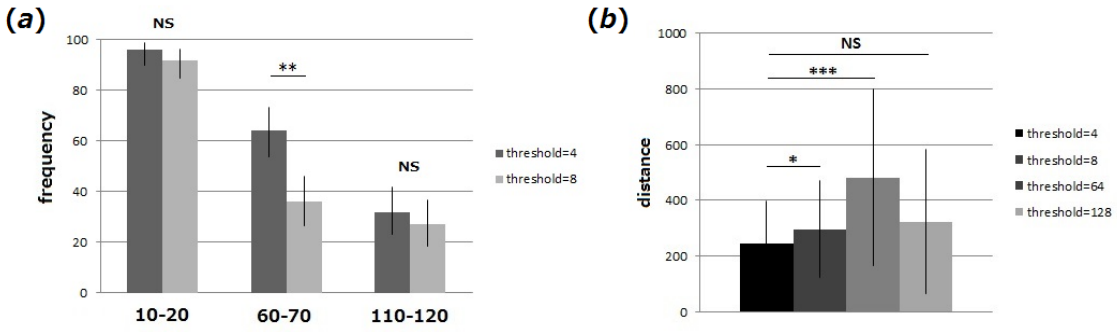

Figure 6. (*a*) Frequency of successfully reaching one of the feeder sites in 10,000 steps for each of the threshold values (θ=4, 8) when the REV-Random algorithm is run for 100 trials. (*b*) Average distances between the start point (origin) and end point in each trial for each threshold value (θ=4, 8, 64 and 128) when the REV-Random algorithm is run for 100 trials. Straight lines indicate error bars. *P<0.05, **P<0.001, NS indicates not significant.

2-1-4. DISCUSSION

Our results indicate that a flexible random walk similar to a Lévy walk will be achieved using probability intervals that change based on the agent's history and that have a uniform step length distribution. As mentioned above, this algorithm results in super-diffusion. Therefore, it will be possible to attain long-range exploratory efficiency [5, 17]. Although we assumed a very low food density in our simulations, the important result is that efficiency was achieved through a balance between near and distant areas. Effective long-range models, such as the Lévy walk model, are not actually very suitable for searching high-target-density and range-limited areas [15].

In our algorithm, the current probability intervals change depending on an agent's own experiences. The agent only knows its most recent four random numbers concretely. Based on this event history, the agent experiences directionally biased movement. If the number of consecutive steps in the same direction reaches the threshold value, the current probability intervals are changed. At this moment (the tth step), the values of $R(t\text{-}3)$ to $R(t\text{-}1)$ are based on the probability intervals defined by the previous rule, and only $R(t)$ is free from these intervals (e.g., $R(t\text{-}3) \in I_0(\text{t-}1)$, $R(t\text{-}2) \in I_0(\text{t-}1)$,

$R(t\text{-}1) \in I_0(\text{t-}1)$ and $R(t) \in I_1(\text{t-}1)$). Therefore, using these four numbers provided by chance, the agent takes a new step associated with new probability intervals. Thus, the agent's move forward is biased. However, the accumulating directional bias causes the probability intervals to change at a higher frequency. When the direction of movement is biased, it implies that one of the four probability interval regions is larger than the others. Therefore, the range of random numbers that fall within that region is large. Thus, the avoidance of dominance of one region over the others is achieved upon the next interval change, which occasionally produces local areas of concentrated presence. We obtain a power-law distribution based on the distribution of time intervals between interval change events. By altering the rule and taking the next step with ambiguity, the agent can involve the world actively. However, the agent cannot change the rule with complete freedom. Instead, he produces directional inequality by choosing a direction using limited information provided by chance. Thus, having to take such an action as a result of chance might be associated with achieving effective exploration.

In our algorithm, the agents only have knowledge of the most recent four random numbers determining their movement. Thus, the algorithm does not require agents to necessarily have high-performance memory abilities. By deviating from one-to-one behavior with respect to a certain fixed rule, i.e., a simple diffusion-predictive moving frame, it is possible for the agent to display behavior beyond a predictive frame, i.e., to achieve super-diffusion. Therefore, our algorithm could represent an abstract explanation for biological phenomena focusing on an agent's degree of activity. It was recently reported that the nest-searching behavior of foraging ants corresponds to a Brownian walk [19]. However, in some species of insects and fishes, searching behavior changes in response to certain environmental alterations linked to extinction, e.g., the amount of available food [20,21]. In fact, ants show different searching behaviors depending on the relevance of the visual information provided to them [22]. Dramatic behavioral changes caused by the agent's involvement and interactions with the environment and other agents, such as nestmates, might be possible [13,22,23]. Balancing an agent's own degree of activity and passivity based on limited available information will achieve such flexible behaviors [24].

2-2 The relationship between “randomness” and “power-law” on Lévy-like foraging

2-2-1. BACKGROUND

Two major issues in an agent’s moving strategies are commonly discussed. One is deterministic walk problems, which occur when the agent has complete location information, such as which position is suitable for establishing effective reach [1, 2]. The other type is known as random walk problems, in which the agent does not have any location information. Therefore, the problem is to determine which probability distribution, such as the Lévy or Brownian walk, can provide effective exploration in certain situations and empirical studies showing Levy and Brownian walks by individual animals are also conducted [3-11, 23].

From one point of view, the former indicates a closed world for the agent in terms of the knowledge that is already acquired by the agent and the one-to-one correspondence between the position of the agent and every fixed location; this information comprises the inner map of the agent. There is no interaction between the agent and unknown environments. In contrast, the latter indicates an open world for the agent in terms of its absolute acceptance of the direction or move length of the next time step. The agent has no location information available about its own relative position and must therefore accept the direction or move length defined by a given fixed probability distribution for each time step. Thus, for each time step, there is a one-to-one correspondence between the position of the agent and next move position. Repeating this simple action, the agent could arrive at its destination, such as a feeder site or its own nest [25, 26]. These two main issues (deterministic and random walk algorithms) are therefore mutually exclusive.

In a recent study, we proposed an effective new random walk algorithm, called the REV algorithm, in which the agent alters the next moving direction and the rule that controls the agent's movement based on its own biases in its moving direction [27].

In the REV algorithm, the agent changes the current rule using the most recent four random numbers if it experiences directional biases in its movement, such as “$+x$, $+x$, $+x$, $+x$”, and if this bias exceeds the threshold value (see [27] for more details). Of the four random numbers, ($R(t)$, $R(t\text{-}1)$, $R(t\text{-}2)$, $R(t\text{-}3)$), only $R(t)$ is independent of the previous random region when the rule changes; thus, only $R(t)$ is a non-bounded number. Therefore, the agent changes the rule using these four random numbers. On the one hand, as the current rule is changed, the agent accepts this non-bounded $R(t)$ to some degree. On the other hand, however, the agent does not accept $R(t)$ absolutely; instead, the agent moves in a new direction that combines this non-bounded number “$R(t)$” with the three

bounded numbers from $R(t\text{-}1)$ to $R(t\text{-}3)$. Therefore, the REV algorithm balances "activeness and passiveness" or "a closed world and an open world".

In this paper, we investigated the power of adding a non-bounded number to change the rule. We used two algorithms, the REV algorithm and the REV-bounded algorithm. In the REV-bounded algorithm, all four random numbers that are used to change the rule are bounded. We showed that the REV-bounded algorithm did not have more super-diffusion properties or power-law distributed move lengths than did the REV algorithm and showed the importance of a non-bounded random number in the rule change.

2-2-2. MATERIALS & METHODS

1. Model description

We propose two random algorithms: the REV algorithm and the REV-bounded algorithm. First, we describe the fundamental model of each algorithm.

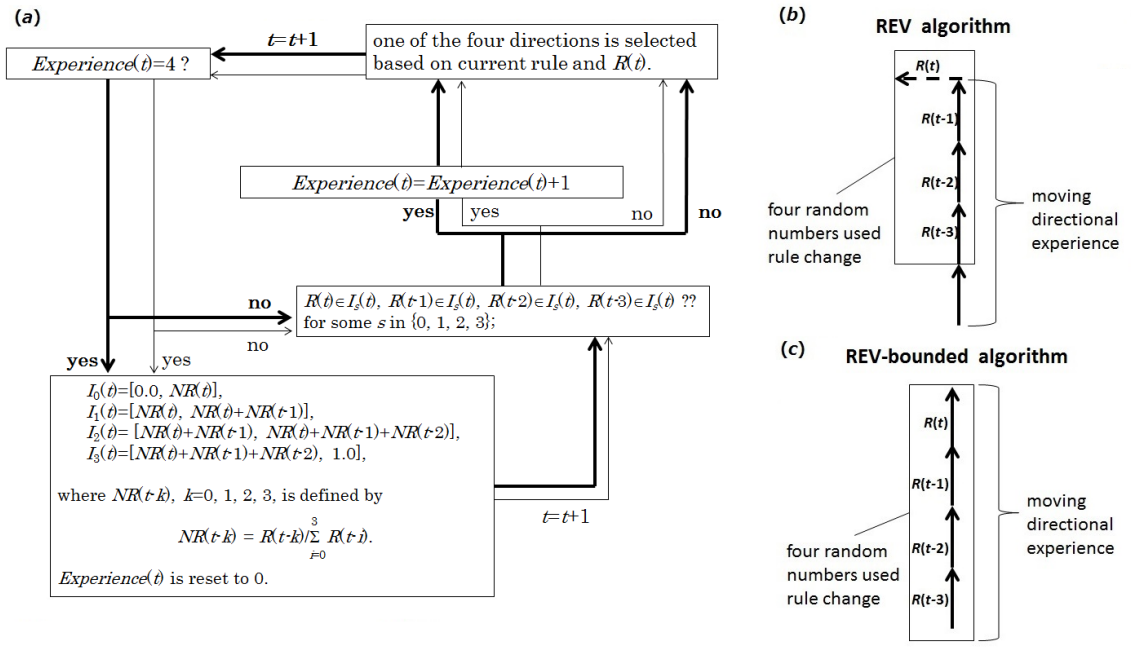

Figure 1. (*a*). Flow chart of the REV algorithm and the REV-bounded algorithm. The bold arrows and letters indicate the REV algorithm. The thin arrows and letters indicate the REV-bounded algorithm. "*Experience*(*t*)" indicates the number of experienced directional movements, such as "*-x*, *-x*, *-x*, *-x*". (*b*) and (*c*). Schematic of four random numbers in the two algorithms. Each arrow represents the movement direction for each time step. "$R(t)$, $R(t\text{-}1)$, $R(t\text{-}2)$, $R(t\text{-}3)$" indicate the four random numbers used for the rule change. (*b*). REV algorithm. $R(t)$ is not bound by the movement directions of the other three random numbers. (*c*). REV-bounded algorithm. All of four random numbers are bounded regarding the movement directions.

1-1. re-valued (REV) algorithm

In our re-valued (REV) random walk model, the agent has a memory at the tth step that allows the agent to access four random numbers, $R(t)$ to $R(t\text{-}3)$. The interval in the REV random walk, $I_s(t)$ for s=0, 1, 2, 3, is changed using the four random numbers when the accumulation of the agent's directional moves exceeds a threshold number. The four intervals are initially set to $I_0(0)$=[0.0, 0.25], $I_1(0)$=[0.25, 0.5], $I_2(0)$=[0.5, 0.75] and $I_3(0)$=[0.75, 1.0]. The next walk is defined by the following equations:

$$(x(t+1), y(t+1)) = (x(t)\text{-}1, y(t)), \text{ if } R(t)\in I_0(t); \quad =(x(t)+1, y(t)), \text{ if } R(t)\in I_1(t);$$
$$=(x(t), y(t)\text{-}1), \text{ if } R(t)\in I_2(t); \quad =(x(t), y(t)+1), \text{ if } R(t)\in I_3(t),$$

Thus, every trial starts as a simple random walk.

A directional move that consists of a series of the same move, such as $-x, -x, -x$, …, is counted as follows:

$$Experience(t+1)=Experience(t)+1, \quad \text{if } R(t)\in I_s(t), R(t\text{-}1)\in I_s(t), R(t\text{-}2)\in I_s(t), R(t\text{-}3)\in I_s(t)$$
$$\text{for some } s \text{ in } \{0, 1, 2, 3\};$$
$$Experience(t+1)=Experiene(t), \text{ otherwise.}$$

For example, a directional move by the agent from t-3 to t that corresponds to a $-y$, $-y$, $-y$, $-y$ series implies the following:

$$R(t)\in I_3(t), R(t\text{-}1)\in I_3(t), R(t\text{-}2)\in I_3(t), R(t\text{-}3)\in I_3(t)$$

Therefore,

$$Experience(t+1)=Experience(t)+1$$

However, a directional movement by the agent from t-3 to t that corresponds to $+x$, $+y$, $+y$, $+y$ implies the following:

$$R(t)\in I_3(t), R(t\text{-}1)\in I_1(t), R(t\text{-}2)\in I_3(t), R(t\text{-}3)\in I_3(t)$$

Therefore,

$$Experience(t+1)=Experience(t)$$

If $Experience(t)$ exceeds a threshold number, θ, the four intervals are changed as follows:

$$I_0(t)=[0.0, NR(t)], \qquad I_1(t)=[NR(t), NR(t)+NR(t\text{-}1)],$$

$I_2(t)$= [$NR(t)$+$NR(t$-1), $NR(t)$+$NR(t$-1)+$NR(t$-2)], $I_3(t)$=[$NR(t)$+$NR(t$-1)+$NR(t$-2), 1.0],

where $NR(t-k)$, k=0, 1, 2, 3, is defined by

$$NR(t-k) = R(t-k)/\sum_{i=0}^{3} R(t-i).$$

When *Experience(t)* exceeds θ, *Experience*(t) is reset to 0.

For example, if *Experiences*(t) exceeds threshold number θ and recent four random numbers are given like followings,

$R(t$-3)=0.10,
$R(t$-2)=0.20,
$R(t$-1)=0.20,
$R(t)$=0.10

Then, $I_s(t)$, s=0,1,2,3 are changed to following equations.

$I_0(t)$=[0.0, 0.17]
$I_1(t)$=[0.17, 0.50]
$I_2(t)$=[0.50, 0.83]
$I_3(t)$=[0.83, 1.00]

Therefore, if $R(t$+1)=0.20 on next time, the agent can go forward along +x.

In our simulations, θ is set to 4 in both algorithms.

1-2. REV-bounded algorithm

The description of the REV-bounded algorithm is the same as that for the REV algorithm except for the timing of "t=t+1" (Figure 1*a*). In the REV algorithm, $R(t)$ is independent of the previous random regions. For example, the following could occur when the current rule is changed.

$R(t)\in I_r(t)$, $R(t$-1$)\in I_s(t)$, $R(t$-2$)\in I_s(t)$, $R(t$-3$)\in I_s(t)$

where $r \neq s$

Therefore, $R(t)$ could be bigger or smaller value extremely than the other three numbers.

In the REV-bounded algorithm, however, the following must occur when the current rule is changed.

$R(t)\in I_s(t)$, $R(t$-1$)\in I_s(t)$, $R(t$-2$)\in I_s(t)$, $R(t$-3$)\in I_s(t)$

In this regard, $R(t)$ is non-bounded in the REV algorithm but bounded in the REV-bounded algorithm (Figure 1*b* and 1*c*).

2-2-3. RESULTS

It appears that both algorithms show directionally biased movement while also forming local spots to some degree (Figures 2*a* and 2*b*).

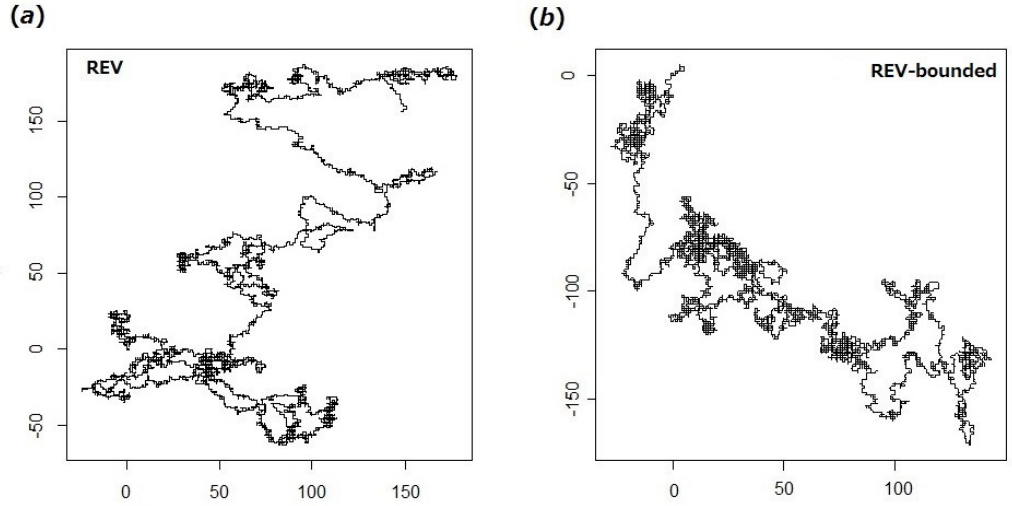

Figure 2. Example of the trajectories in the two algorithms. (*a*). REV algorithm. (*b*). REV-bounded algorithm. The agent starts at the origin in each trial.

We evaluated whether the food exploration efficiencies differ between the algorithms. We set four fixed food locations with a size of 10×10 grids that were located at the 10-20, 60-70 and 110-120 positions on each of the axes. The 10-20 position indicates that each of the four food areas was located between 10 and 20 units from the origin on one of the axes. Figure 3 shows the similar results of the two algorithms regarding the success frequencies for finding one of the food locations (Figure 3*a*). The success of finding food is defined by the agent's arrival at one of the food locations (REV vs. REV-bounded, 10-20; n=97 vs. n=98 out of 100 trials, Fisher's Exact Test, P=1.00, NS, 60-70; n=52 vs. n=55 of 100 trials, chi-squared test, χ_2^2=0.08, P=0.78, NS, 110-120; n=36 vs. n=24 of 100 trials, chi-squared test, χ_2^2=2.88, P=0.09, NS). However, the REV algorithm searched more efficiently in terms of the time to reach the food (Figure 3*b*) (REV vs. REV-bounded, 10-20; $MEAN_{REV}$=218.8±558.63, $MEAN_{bounded}$=220.10±353.79, Mann-Whitney U test, U=4410.00, P=0.38, NS, 60-70; $MEAN_{REV}$=2835.00±2248.32, $MEAN_{bounded}$=3650.00±2135.73, Mann-Whitney U test, U=1025.00, P<5.00E-02, 110-120; $MEAN_{REV}$=3896.00±2102.64, $MEAN_{bounded}$=5897.00±2304.52, Welch Two Sample t-test, t=-3.41, df=46.26, P<5.00E-03). The agent can reach food areas faster using the REV algorithm than using the REV-bounded algorithm for food that is far from the starting

point, indicating REV algorithm is more suitable for food searching at least when resources are sparsely distributed. The mean squared displacement and the time step of the REV algorithms follow a super-diffusion process, i.e., the following relation is achieved [27].

$$\langle R^2 \rangle \sim t^{2H},\ H>0.5$$

H=0.5 corresponds to a Brownian walk [15, 17].

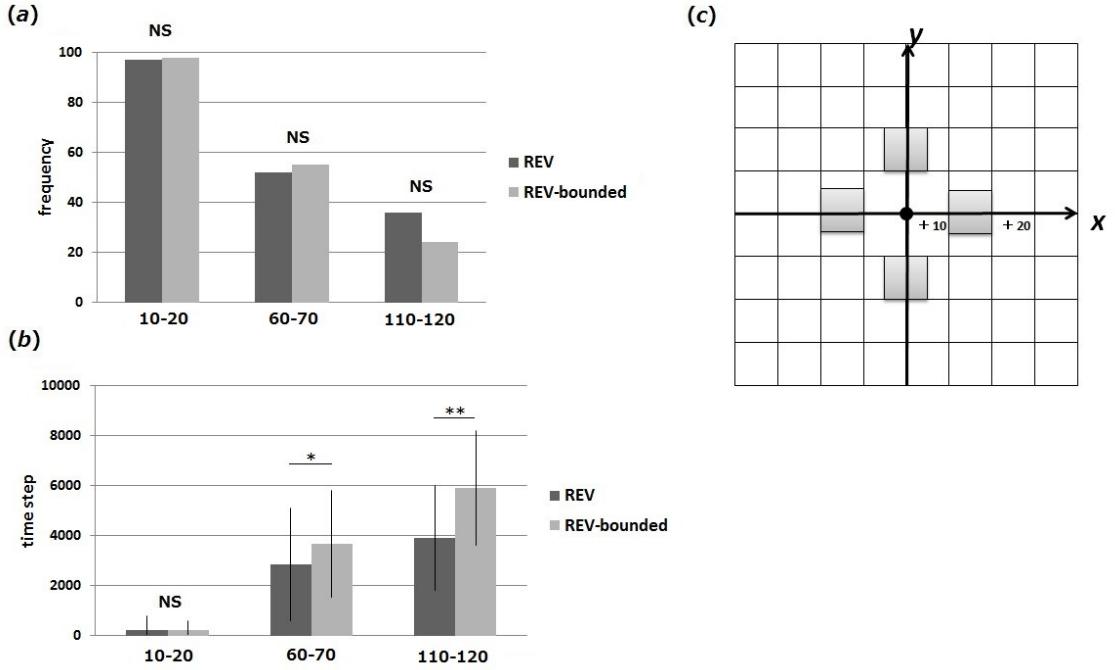

Figure 3. Success frequencies and time steps to reach one of four food locations within 10,000 time steps. (*a*). Frequencies for three versions. The 10-20 designation indicates that each of the 10×10 grid-sized four food areas is located between 10 and 20 units from the origin on one of the axes. (*b*). Time steps used to reach one of the food locations within 10,000 time steps for the three versions. (*c*) Schematic of four food locations. Here, the 10-20 versions are plotted. Gray squares indicate food areas. The black dot located at the center indicates the origin. The size of each lattice is 10×10. **P*<0.05, ***P*<0.01, *NS*: non-significant. The vertical lines indicate error bars.

Figure 4 shows that the REV-bounded algorithm does not show any super diffusion (R-squared=0.99, slope=0.29<0.50, we obtained each value at time points of 500, 1000, 1500, … using 1,000 trials). This finding is opposite to that of the REV algorithm, which shows super diffusion [27]. We also evaluated whether the agent's log-scale move lengths followed power-law distributions or exponential-law distributions (Figures 5 and 6). In this paper, the move step lengths were defined as follows. Any 180° turn that occurred within 2.5 distances was considered a saccade turn. The step length (>1.00) was considered the shortest distance between any two sequential saccade turns (Figure 5*d*). Figures 5*a* and 5*b* show examples of log-scale plots of the step lengths

and cumulative distributions from one trial of each algorithm. We conducted 20 trials for each algorithm and obtained the average slopes (μ). Figure 5*c* shows that the μ of the REV algorithm is closer to 2.00 than that of the REV-bounded algorithm, indicating that the REV algorithm is more suitable for food searching (mean μ_{REV}=2.68±0.068, mean $\mu_{bounded}$=2.88±0.069, Welch Two Sample t-test, t=-9.44, df=37.99, P<1.0E-10) [28]. Figure 6*a* shows the frequencies of the AIC weights of power-law, here we denoted it as "$w(p)$" values. We could determine the frequencies of each algorithm by conducting 20 trials for each. As seeing in figure 6*a*, there were significant differences of the values of $w(p)$'s variances between two algorithms (σ^2_{REV}=0.050, $\sigma^2_{boudned}$=0.166, Bartlett's test, χ_2^2=6.39, df=1.00, P<5.0E-2.0). Moreover, the $w(p)$ values are higher in the REV algorithm than in the REV-bounded algorithm (Figure 6*b*) (mean $w(p)_{REV}$= 0.95±0.22, mean $w(p)_{non\text{-}ref}$=0.79±0.41, Mann-Whitney U test, U=149.00, P<5.0E-2). G-test was used to check whether each trial data was fitted to the best model and each data was fitted to the model, excepting two trials from REV-bounded algorithm (G=53.62, df=2, P<1.00E-11, G=27.42, df=2, P<1.0E-5). These results indicate that the $w(p)$ of the REV algorithm appears to be more consistent and reach higher amplitudes than that of the REV-bounded algorithm.

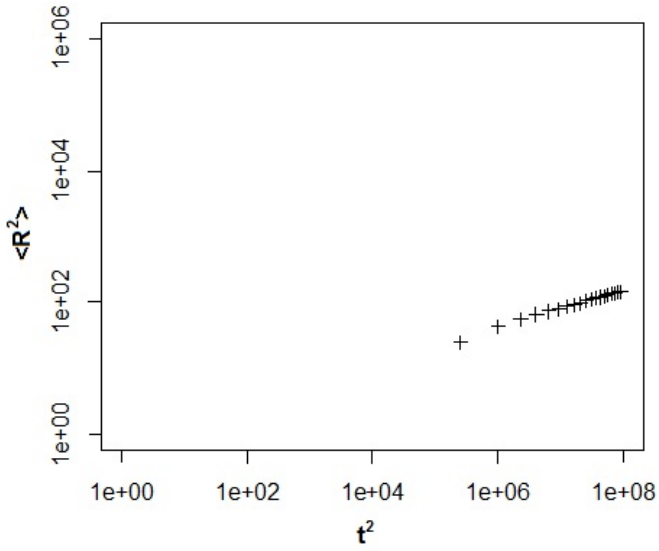

Figure 4. Log-scale plot of the mean squared displacement and the squared time of the REV-bounded algorithm

We also calculated step lengths defined as displacements between any consecutive trajectory points from 1 trial in REV algorithm [29]. We obtained each trajectory point at 10 time step intervals for each direction (X and Y) and estimated whether step lengths followed power-law distributions or exponential ones. Results are shown in Table S1. We could obtain that only step lengths regarding to Y direction showed power-law distributions ($w(p)_X$=0.00, λ_X=0.70, $w(p)_Y$=1.00, μ_Y=2.76).

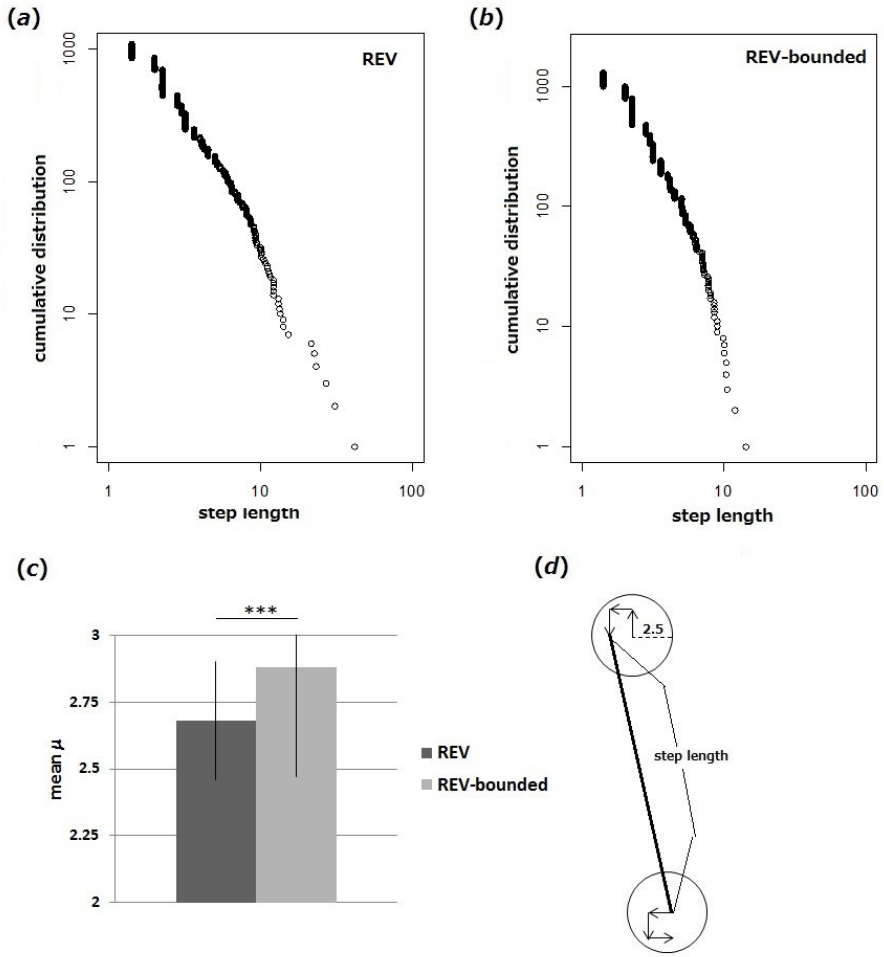

Figure 5. Log scale of the step lengths and the cumulative distributions for each algorithm from one trial. (*a*). REV algorithm. (*b*). REV-bounded algorithm. (*c*). Mean μ values of each algorithm from 20 trials. (*d*). Schematic of the definition of step length. The bold black line indicates the step length. Each circle indicates a saccade turn region, which has 2.5 distances. Each arrow indicates the agent's trajectory for a time step. ***P<0.001. The vertical lines indicate error bars.

2-2-4. DISCUSSION

We proposed two random walk algorithms. Both algorithms clearly exhibited directional biases in the movements. Actually, there was no difference in the number of successful arrivals to food sites between these two algorithms. However, our results indicate that not only the change in the current rule but also partial randomness are important to achieve effective food searching distributed sparsely in terms of the time spent to reach food areas and the emergence of consistent power-law distributions. An agent using the REV algorithm could reach a feeder site faster than one using the REV-bounded algorithm. The log-scale move lengths and the cumulative distributions of the REV

algorithm also showed more reliable power-law distributions than those of the REV-bounded algorithm. By conducting another method, we could obtain power-law distributed step lengths regarding to only Y direction in 1D. Perhaps, the agent's fixed and discrete movement step and speed might affect our results regarding to step lengths calculation methods [29].

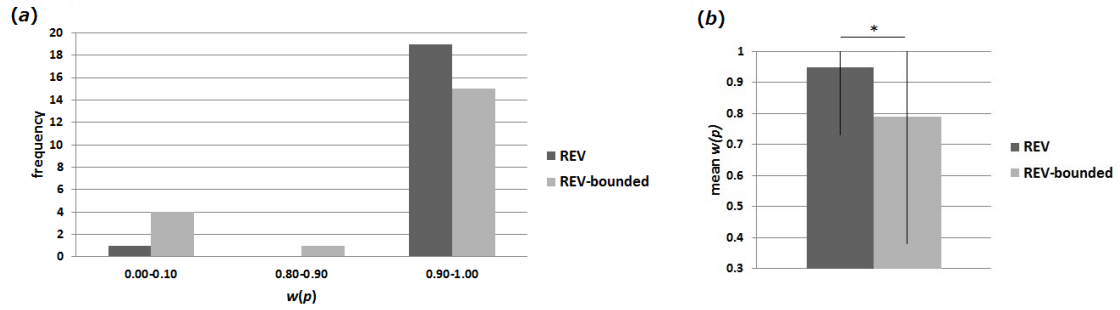

Figure 6. Distribution of AIC power-law weights ($w(p)$) and AIC exponential-law weights from 20 trials. (*a*). Frequencies of $w(p)$ distributions for 20 trials. Note that the frequencies of $w(p)$ from 0.10-0.80 were 0 in both algorithms. (*b*). Mean $w(p)$ values from 20 trials of the two algorithms. *$P<0.05$. The vertical lines indicate error bars.

In both algorithms, the agent changes the rule using the most recent four random numbers, $R(t)$ to $R(t\text{-}3)$, if it experiences directional biases in its movement and if those biases exceed a threshold value. In the REV algorithm, R(t) is non-bounded, i.e., the following could occur:

$$R(t)\in I_r(t),\ R(t\text{-}1)\in I_s(t),\ R(t\text{-}2)\in I_s(t),\ R(t\text{-}3)\in I_s(t),$$

where $r \neq s$.

Therefore, $R(t)$ provides agents with absolute "randomness" in their movement directions because $R(t)$ differs from the other three bounded numbers, $R(t\text{-}1)$, $R(t\text{-}2)$ and $R(t\text{-}3)$. Agents accept this number to a certain degree, and an agent could then change the rule by combining this number with the other bounded numbers. Thus, a balance between passive and active and between a topological or flexible map must be achieved in this algorithm.

In contrast to the REV algorithm, the REV-bounded algorithm only provides bounded numbers to agents. In this case, the power-law distributions of log-scale step lengths are inconsistent, and the variances are high. Sometimes, the weight of the exponential law exceeded the weight of the power law. Thus, adding a random number to the rule change appears to play an important role in the emergence of consistent power-law distributions. All four bounded numbers in REV-bounded algorithm indicate the past numbers. Therefore, the rule would be determined by established numbers. In this sense, this algorithm might be considered as Monrovian process, differing from REV algorithm in which non-bounded number is used to change the rule.

Recently, animal moving strategies were reported to differ based on the context [13, 14 and 23]. However, little is known about the origin of power-law movements, such as the Lévy walk [23 27,

30-32]. Our models might be applied to animal searching behavior in complex environments, for example, in which obstacles are installed. The agent must produce unpredictable movements by interacting outside environments. Previously acquired knowledge and ignorance about food locations or unknown environments are generally considered to be mutually exclusive. However, these factors could coexist while also showing power-law distributions.

2-3 Weber-Fechner relation derived from interactions in random walk strategy

2-3-1. BACKGROUND

The analysis of the random strategies of animals is often studied with algorithms by matching their living movements and to the results of simulations [4-7,9,10,17]. Some studies have reported that animals have exhibited a Lévy Walk rather than a Brownian Walk [23, 33-36]. However, animal movement might be context-dependent [13, 14].

The fundamental problem with studying animal foraging behavior is how to achieve optimal searching without assuming a power-law distribution. A robust algorithm should not only optimize a random walk, but should also estimate how these flexible behaviors arise from the individual activities of each agent [15].

A Lévy distribution is defined as a process whereby an agent takes steps of length l at each time, where l is a probability density distribution with a power-law tail:

$$P(l) \sim l^{\mu}$$

with $1<\mu \leqq 3$. A Lévy walk with $\mu \approx 2$ shows effective random searching in environments with randomly distributed food sites which are non-destructive [5, 28]. For $\mu>3$, the Lévy walk converges to Brownian motion.

The Weber-Fechner relation is the linear relation between physical magnitudes of input stimulus and subjective perceived intensity and sometimes discussed as one of origin of power-law distributions [37-40]. However, no studies have reported how these two equations would be emerged together. How can we achieve the Weber-Fechner equations related to power-law distributions? Here, we describe how these two equations are obtained on agent simulations. Subjective perceptions depending on physical magnitude of input information might be produced by agents' subjective interpretations. Therefore, deviation of Gaussian distributed errors of input information would emerge as subjective output. We developed a random walk algorithm using multi-agent model and tackled on the origin of Lévy walk which had power-law tailed distribution. The relationship between the Weber-Fechner law and Lévy movement is also studied as random walk problems [40].

Recently, we proposed a random walk algorithm called re-valued algorithm, in which the agent has a limited memory capacity (i.e., only a memory of four recent random numbers) [27, 41]. Using these random numbers, the agent changes its directional rule if the agent experiences moving directional biases. If the agent could observe its entire trajectory while maintaining unbiased random searching, then there would be no need to change the rule because some directional biases only occur probabilistically. However, in a re-valued algorithm, the agent is not able to observe its entire

trajectory but is only aware of a limited trajectory. Therefore, to modify directional biases which are occupied by its current rule, the agent changes its directional rule by producing a correct or erroneous directional interpretation of a few random numbers, resulting in more biased movements that deviate from Brownian motion.

Here, we introduce a new multi-agent random walk algorithm by using a re-valued algorithm as a base simulation model. In this paper, the limitation number of recent random numbers varies depending on the interactions between agents. Through local interactions, agents change their limitation number as well as their directional rule as in the original re-valued algorithm. We show that in our new algorithm, the Weber-Fechner law and a power-law distribution would be driven as a consequence of the step lengths. Later, we discuss the implications of our results.

2-3-2. MATERIALS & METHODS

1. Model description

We propose new random walk algorithm based on original re-valued (REV) algorithm [27, 41]. In our new model, multi agents are in the same simulation field and through local interactions, every agent changes its own directional bias length. We describe the details of our new algorithm as followings.

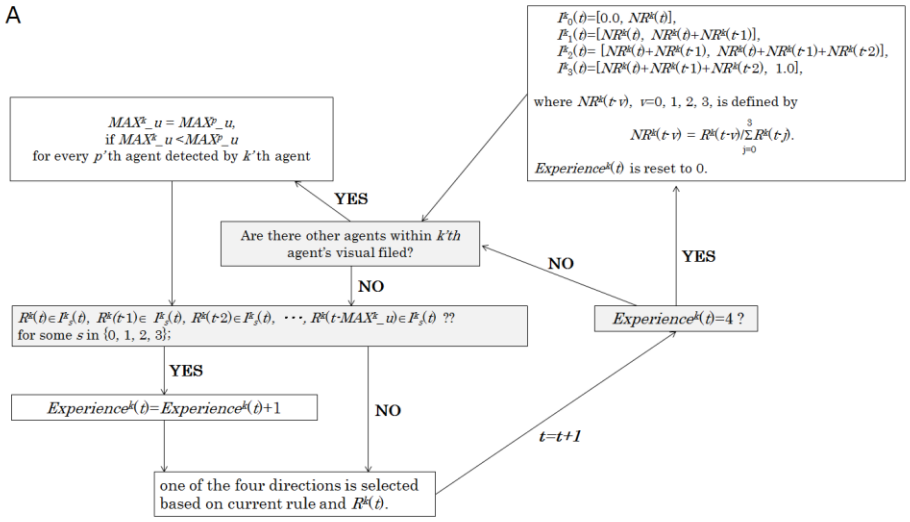

Figure 1. Flowchart of our algorithm and explanation of rule change events. A. Flowchart of our algorithm. $I_{0,k}$, $I_{1,k}$ $I_{2,k}$, $I_{3,k}$ are directional rules for k'th agent. $R^k(t)$ indicates the random number at the tth step for kth agent. $Experience^k(t)$ indicates the experience number for directional biases for kth agent. Note that grey zones indicate the zones in which agents must determine the choice depending on situations. B. Schematic explanation of rule change events in case of $MAX\_u = 3$ as an example. Note that time step value is changed before rule change events.

1-1.multi- re-valued (multi-REV) algorithm

In our multi- re-valued (multi-REV) random walk model, we set 500 agents in 500×500 grid size field. Each agent moves on two dimensional lattices with step length 1 on each time step. The kth agent has a memory at the tth step that allows the agent to access four random numbers, $R^k(t)$ to $R^k(t\text{-}3)$, and updates the interval in the multi-REV random walk, $I^k_s(t)$ for s=0, 1, 2, 3, which is employed to a weighted dice. The $I^k_s(t)$ is changed using the four random numbers when the accumulation of the agent's directional moves exceeds a threshold number. The four intervals are initially set to

$$I^k_0(0)=[0.0, 0.25],\ I^k_1(0)=[0.25, 0.5],\ I^k_2(0)=[0.5, 0.75] \text{ and } I^k_3(0)=[0.75, 1.0],$$
$$\text{for all } k\text{th agents}$$

The next walk is defined by the following equations:

$$(x^k(t+1), y^k(t+1)) = (x^k(t)\text{-}1, y^k(t)), \text{ if } R^k(t)\in I^k_0(t); \quad =(x^k(t)+1, y^k(t)), \text{ if } R^k(t)\in I^k_1(t);$$
$$=(x^k(t), y^k(t)\text{-}1), \text{ if } R^k(t)\in I^k_2(t); \quad =(x^k(t), y^k(t)+1), \text{ if } R^k(t)\in I^k_3(t),$$

Thus, every trial starts as a simple random walk.

A directional move that consists of a series of the same move, such as $-x, -x, -x, \ldots$, is counted as follows:

$$Experience^k(t+1)=Experience^k(t)+1, \quad \text{if there exists } s \text{ in } \{0, 1, 2, 3\} \text{ such that } R^k(t\text{-}m)\in I^k_s(t) \text{ for all } m \text{ in } \{0,1,\ldots, MAX^k\_u\};$$
$$Experience^k(t+1)=Experiene^k(t), \quad \text{otherwise.}$$

MAX^k_u is assigned to every agent as initial condition by choosing one value randomly such as

$$MAX^k\_u \in \{2,3,4,5\}$$

For example, if $MAX^k\_u = 5$ and directional move by that agent from t-5 to t that corresponds to a $-y$,

-y, *-y*, *-y, -y, -y* series implies the following:

$$R^k(t)\in I^k_3(t),\ R^k(t\text{-}1)\in I^k_3(t),\ R^k(t\text{-}2)\in I^k_3(t),\ R^k(t\text{-}3)\in I^k_3(t),\ R^k(t\text{-}4)\in I^k_3(t),\ R^k(t\text{-}5)\in I^k_3(t)$$

which results in

$$Experience^k(t+1)=Experience^k(t)+1.$$

In contrast, a directional movement by that agent from t-5 to t that corresponds to *+y, +x*, *+y*, *+y, +y, +y* implies the following:

$$R^k(t)\in I^k_3(t),\ R^k(t\text{-}1)\in I^k_1(t),\ R^k(t\text{-}2)\in I^k_3(t),\ R^k(t\text{-}3)\in I^k_3(t),\ R^k(t\text{-}4)\in I^k_3(t),\ R^k(t\text{-}5)\in I^k_3(t)$$

which results in,

$$Experience^k(t+1)=Experience^k(t).$$

If $Experience^k(t)$ exceeds a threshold number, θ, the four intervals are changed as follows:

$$I^k_0(t)=[0.0,\ NR^k(t)],$$
$$I^k_1(t)=[NR^k(t),\ NR^k(t)+NR^k(t\text{-}1)],$$
$$I^k_2(t)=[NR^k(t)+NR^k(t\text{-}1),\ NR^k(t)+NR^k(t\text{-}1)+NR^k(t\text{-}2)],$$
$$I^k_3(t)=[NR^k(t)+NR^k(t\text{-}1)+NR^k(t\text{-}2),\ 1.0],$$

where $NR^k(t\text{-}v)$, v=0, 1, 2, 3, is defined by

$$NR^k(t\text{-}v) = R^k(t\text{-}v)/\sum_{i=0}^{3} R^k(t\text{-}i).$$

When $Experience^k(t)$ exceeds θ, $Experience^k(t)$ is reset to 0. In our simulations, θ is set to 4 for all agents.

In addition to individual directional bias experiences, every agent updates its own *MAX_u* value, which is the length of trail regarded as "one step", through local interaction. If the *MAX_u* value increases with local interactions, the agent could hold current directional rule. In our model, every agent has visual detection filed which has 6.0 diameters. If other agents are within *k*th agent's visual field (< 6.0), then *k*th agent change its own *MAX_u* value by:

$$MAX^k\_u = MAX^p\_u, \text{ if } MAX^k\_u < MAX^p\_u$$

for every pth agent detected by kth agent

Thus, if more than single agent is detected by kth agent, then, MAX^k_u value is reset to other agent's value which has maximum MAX_u value among detected agents for kth agent. We defined each trial state as a steady state if all agents have same MAX_u value, i.e., all agents have $MAX\_u = 5$. On each trial, simulation state converged to steady state by approximately 3,000 time steps. See also Figure 1A and 1B for flowchart of our model.

2-3-3. RESULTS

Figure 2 indicates some agents' trajectories from 1 trial. It seems that agents tend to show deviated movements from Brownian motions. First we investigated whether step lengths exhibit Weber-Fechner relation or not. In this paper, we defined the step lengths as the shortest distances between consecutive two saccade turns. We regarded turns as saccade turns if agents make 180°turn within 5.0 diameters. Thus we regarded step lengths at the distance of 5.00 as the smallest step lengths in this paper. Figure 3 shows that relation of mean lengths, $l_{n,}$ (>= 5.00) and mean absolute differences between consecutive step lengths, $|l_{n+1} - l_n|$. We obtained mean absolute differences by setting the bin width as 50.00 conducting 2 trials until steady states. According to Figure 3, there is a linear relation between them. The more step lengths l_n are longer, the more absolute differences between consecutive step lengths are longer (y=0.92x-2.17, R-squared = 0.98). This result indicates that Weber-Fechner law is achieved in our simulation regarding to step lengths.

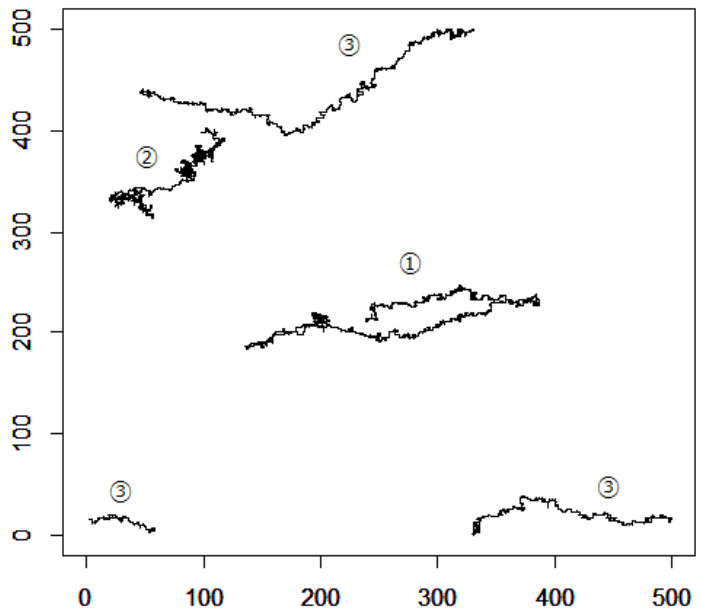

Figure 2 Example of agents' trajectories from 1 trial. Here three agents' trajectories are plotted. Each number indicates each agent's trajectory.

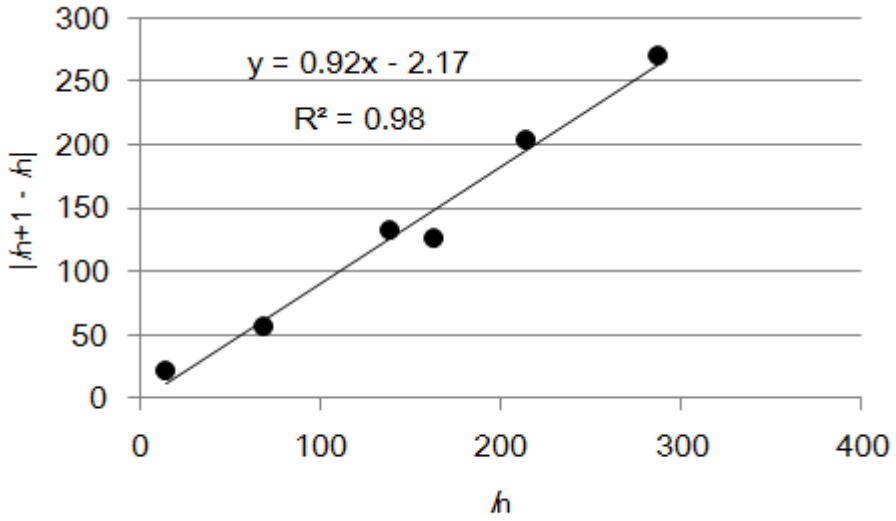

Figure 3. The relation of mean lengths, l_n, (>= 5.00) and mean absolute differences between consecutive step lengths, $|l_{n+1} - l_n|$. We obtained mean absolute differences by setting the bin width as (0-50,50-100,⋯). These data were obtained and summed up from 2 trials.

Figure 4A shows log-log scale cumulative distribution of step lengths obtained from all agents. We stopped the simulation to obtain the step lengths when the simulation reached to steady state and obtained agents' trajectories every 10 time steps. These data were obtained from 10 agents from 1 trial. Agents in our algorithm show power-law tailed movements with scale of almost two-decades (Figure 4A, N of data=54, AIC weight of power-law =1.00 against AIC weight of exponential-law (=0.00). μ=1.90. G-test: G-squared = 0.93, df = 4, P= 0.92, NS). We also evaluated whether super-diffusion property is maintained or not. Log-log scale plot of $<R^2>$ and t^2 are shown in Figure 4B, indicating that property is achieved. We obtained the data every 100 time steps by conducting 6 trials. The inset is an expansion graph showing the ten largest values (slope=0.85, R-squared=0.99 (slope=0.55, R-squared=0.97 in case of inset data)).

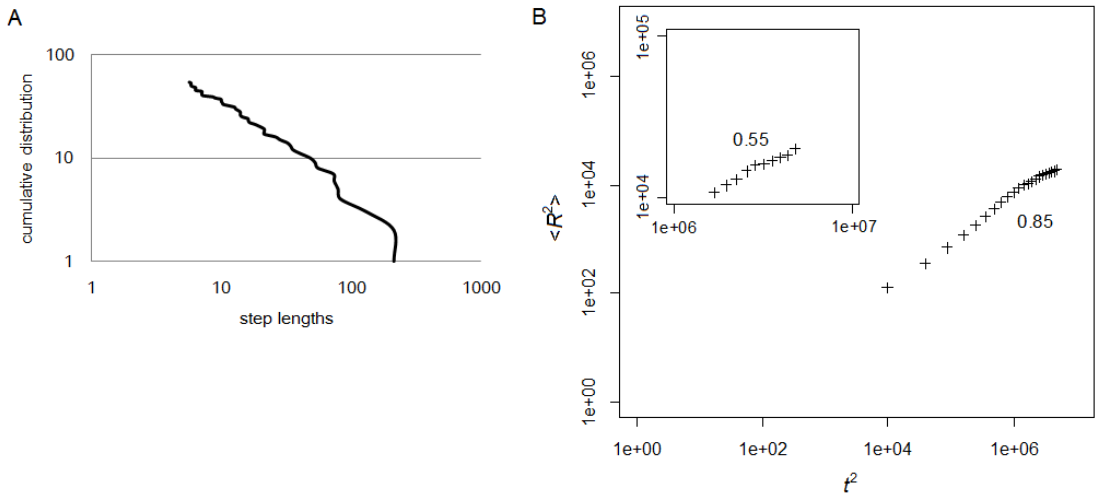

Figure 4. A. Log-scale plots of step lengths (>= 5.00) and that of cumulative distribution by conducting interacting algorithm until steady state. Step lengths were defined as shortest distances between consecutive saccade turns. Here, saccade turn was regarded as agents made 180°turn within 5.00 diameters. We obtained agents' trajectories every 10 time steps. These data were obtained from 10 agents from 1 trial. We stopped calculation when state reached to steady state. *N* of data=54, AIC weight of power-law =1.00 against AIC weight of exponential-law (=0.00). μ=1.90. G-test: *G*-squared = 0.93, *df* = 4, *P*= 0.92, NS. Dashed line indicates best-fit power-law distribution. B. Log-scale plot of $<R^2>$ and t^2. We obtained data every 100 time steps from 1 trial. The inset is an expansion of the *x*-axis showing the ten largest values. *R*-squared=0.99 (0.97 in case of inset data).

In our algorithm, it seems that agents sometimes make longer step lengths. It will contribute to obtain power-law tailed behaviors. Therefore we evaluated the relationship between velocity and its increment to check how making longer step lengths influenced ensuing moving properties. Recently, it suggests that Langevin equation might contribute to the power-law tailed movements regarding to velocity of simulated agents [30, 42-44]. To estimate the influence of Langevin relation to our algorithm, we show the relation between velocity and velocity increment for x-direction and y-direction respectively (Figure 5A: x-direction, 5B: y-direction). Here, we defined velocity as [displacement / (5 time steps)] and obtained these values from single agent by conducting 1 trial until steady state. There were negative relations between velocity, *u*, and velocity increment, d*u*, in both directions (x-direction: *r*-squared = 0.98, y-direction: *r*-squared = 0.98).

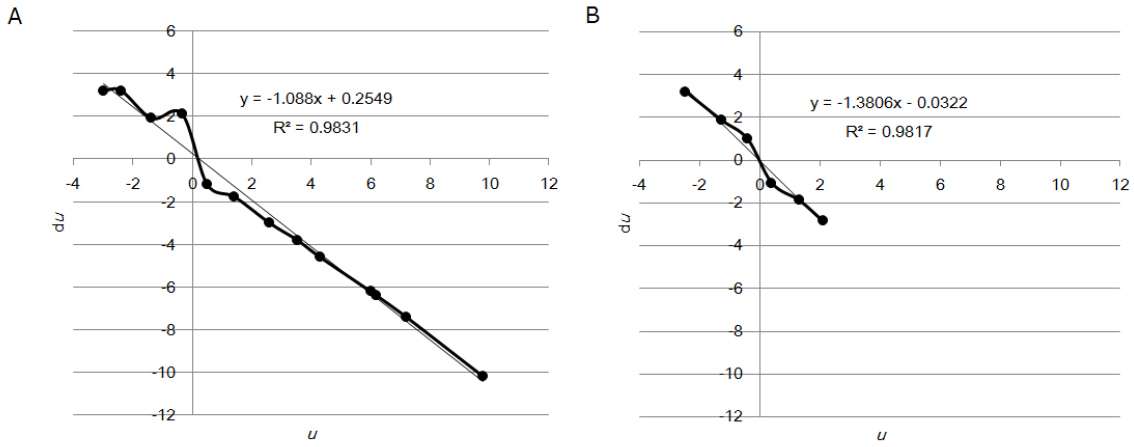

Figure 5. The relation between velocity and velocity increment from single agent by conducting 1 trial until steady state. Here, we defined velocity as [displacement/ (5 time steps)]. A. x-direction. B. y-direction. Averaged data is shown. Bin width is set to 1.00.

.

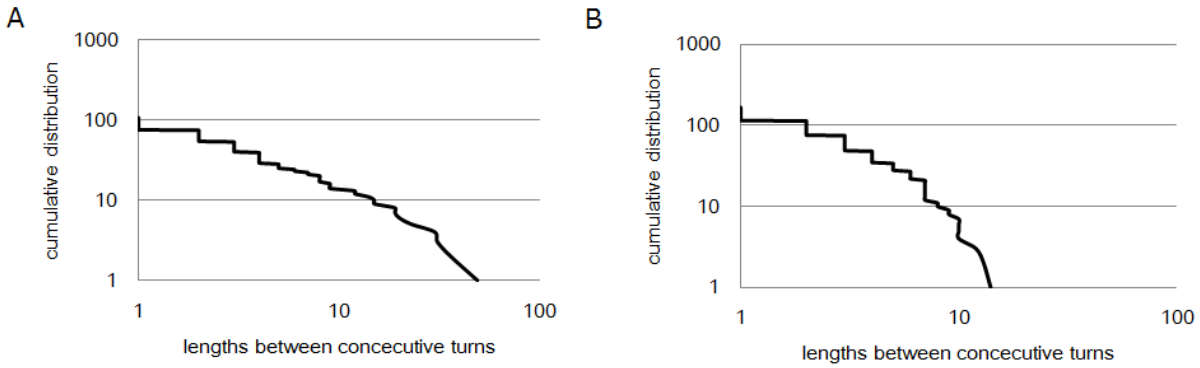

Figure 6. Log-scale plot of step lengths between consecutive velocities' sing change turns for each direction from single agent by conducting simulation run until that state reaching to steady state. A. x-direction. *N* of data=106, AIC weight of power-law =1.00 against AIC weight of exponential-law (=0.00), μ=1.94. G-test: *G*-squared = 1.71, *df* = 4, *P*= 0.79, NS. B. y-direction. *N* of data=167, AIC weight of power-law =1.00 against AIC weight of exponential-law (=0.00), μ=2.17. G-test: *G*-squared = 5.44, *df* =4, *P*= 0.24, NS.

Therefore, we also checked whether step lengths, which were defined as distances between consecutive velocities' sing change points, followed power-law distribution. Figure 6 shows log-scale plot of step lengths between consecutive velocities' sing change turns for each direction from all agents by conducting simulation run until that state reaching to steady state. We could obtain that in both direction, power-law distributed step lengths were achieved (Figure 6A: x-direction. *N* of data=106, AIC weight of power-law =1.00 against AIC weight of exponential-law

(=0.00), μ=1.94. G-test: *G*-squared = 1.71, *df* = 4, *P*= 0.79, NS. Figure 6B: y-direction. *N* of data=167, AIC weight of power-law =1.00 against AIC weight of exponential-law (=0.00), μ=2.17. G-test: *G*-squared = 5.44, *df* =4, *P*= 0.24, NS). In our simulation the slope value (μ) is close to that of step lengths.

Lastly, we checked whether we obtained similar results regarding to power-law distributed step lengths if no agents update *MAX_u* values. We used same algorithm for each agent (500 workers, within 500×500 grid simulation filed) except that *MAX_u* values were fixed to initial values for all agents and no interaction occurred until each trial finished. We set 3,000 time steps as 1 trial because each trial started as steady state. As shown in Figure 7, power-law distribution were no longer achieved regarding to step lengths (*N* of data=63, AIC weight of power-law =0.00 against AIC weight of exponential-law (=1.00). λ=0.055. G-test: *G*-squared = 1.026, *df* = 4, *P*= 0.91, NS).

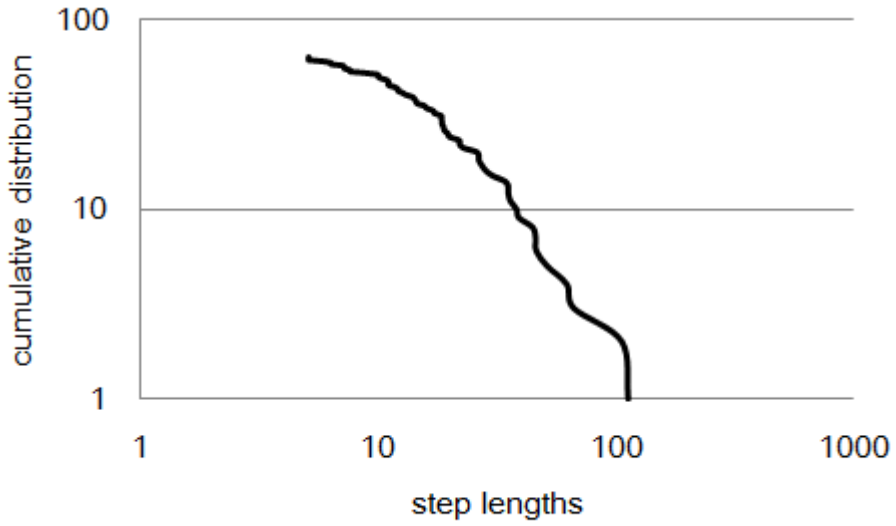

Figure 7. Log-scale plots of step lengths (>= 5.00) and that of cumulative distribution by conducting non-interacting algorithm until 3,000 time steps. Step lengths were defined as shortest distances between consecutive saccade turns. Here, saccade turn was regarded as agents made 180°turn within 5.00 diameters. We obtained agents' trajectories every 10 time steps. These data were obtained from 10 agents from 1 trial. *N* of data=63, AIC weight of power-law =0.00 against AIC weight of exponential-law (=1.00). λ=0.055. G-test: *G*-squared = 1.026, *df* = 4, *P*= 0.91, NS). Dashed line indicates best-fit power-law distribution.

2-3-4. DISCUSSION

We proposed a new random walk algorithm in which multiple agents interact with each other in a limited local visual field, which is based on the original re-valued algorithm for a single agent [27, 41]. If an agent detects some other agents in its own detection field in our algorithm, then that agent

changes *MAX_u* values, directional bias numbers which are employed for the agent, in addition to a rule change occurrence. Power-law distributed step lengths with optimal slope values emerged in our algorithm. There were linear relations between step lengths and absolute differences between those lengths and consecutive ones. Therefore, this relation would follow the Weber-Fechner equation [37, 38].

We also evaluated whether step lengths, which were defined as distances between the change points of consecutive velocities, followed a power-law distribution. We found that viscous-like flows were achieved in our simulation because there were negative linear relationships between velocities and the increments in both directions. The slope values of distances between consecutive turns were close to those of step lengths defined by distances between two saccade turns. Therefore, it seems that super-diffusion movements were achieved while behaving like viscous materials. Agents might modulate viscous parameters by themselves as such materials [25, 45].

We could not obtain any power-law tailed movements when we used a non-interacting algorithm to obtain step lengths. Therefore, it seems that increasing *MAX_u* values is effective for obtaining optimized power-law tailed movements.

In our model, agents use past experiences and recent random numbers to change their behaviors. Depending on bias-experiences, interpretation of measured metric distances would be changed by each agent through rule-change events and biased movements would emerge as a result. In that respect, it might be somewhat related to Bayesian estimation method. Bayesian estimator model is often used to psychological phenomena in which prior distribution and internal measurement are combined to estimate posterior displacement [46-49]. Human behavior approximately follows Weber-Fechner relation [46, 47, 49-51]. Logarithmic internal representation of measured displacement i.e. Weber-Fechner relation is sometimes assumed in this method in order to duplicate experimental results. Further, it seems that power-law equation is also achieved [49].

Without such an assumption, we proposed a model describing micro-level movements, which resulting in achieving Weber-Fechner relation and power-law equation. Why did these results appear? When rule change occurs for an agent, the agent holds ambiguity as to whether the experienced biases should be taken into consideration for a rule change or not. In other words, it might be possible for other agents not to change directional rules depending on their *MAX_u* values even though they experienced the same directional biases as that agent. Therefore, finding other agents in its own detection field and increasing *MAX_u* values would prompt the agent to refine its trajectory and result in the coexistence of subjective and objective biases. Thus, confusing others with it might play an important role [41]. Recently, we proposed a multi-agent model and investigated a possibility of occurrence a cognitive visual illusion. We regarded each agent as each retinal cell or neuron in that paper. Each agent predicted ambiguous global properties through local interactions, resulting in changing its behaviors. Also in this paper, each agent changes its rules by

identifying others into its own past trajectories. Therefore, our model might contribute to explain high-order cognitive phenomena from a micro-level view point.

Agents in our model might always be exposed to uncertainty whether it is right to change rule with experienced series of movement biases or not. The uncertainty of movement biases presented as *MAX_u* values must be modulated through interaction with others. These events could occur independent from a rule change. Therefore, it is possible for some agents to increase their *MAX_u* values before the initial rule change occurs. Thus, the important feature is that agents do not intend to deviate from their initial searching tendencies, i.e., Brownian motion; instead, the agents correct their directional biases to maintain their unbiased searching with respect to direction. However, because their memories are limited, more biased movement would emerge as a result. Agents might achieve flexible behavior by altering the rules in their swarm of local interactions, resulting in emergence of not only a power-law distribution but also an optimized one.

2-4 Lévy-like movements in Japanese carpenter ants

2-4-1. BACKGROUND

It is very important for many animals to achieve a balance between resource exploitation and exploration. This problem has been discussed with respect to ant navigation [24, 52 and 53]. Many ant species recruit their nest-mates using chemical pheromones. Others use tandem or group running. Do followers simply obey recruiters? If this were the case, they would not be able to find new available food. Recruitment would be specialized to exploitation. External noise is known to play a role in new location exploration while specific food locations are being exploited [24]. Without external noise, how can we achieve the necessary flexible balance using internal noise?

Ants appear to lack the ability to use global cognitive maps or locale systems for navigation [26, 54]. Therefore, other local agents' information must contribute in obtaining globally profitable information. It has been shown recently that garden ants might refer to surrounding spaces using other local agents, resulting in global illusion figures [55]. Here, we approach these issues by comparing experiments using Japanese carpenter ants in a random walk model in which agents weakly refer to their surrounding places using other agents' movements and inner noise.

A primary theme of random walk problems is how to achieve Lévy-like movements without assuming power-law tailed distributions, because actual animals show different movement properties depending on environmental contexts [15, 27, 30, 41 and 42]. For example, they might show Lévy walking on one occasion and Brownian walking on another [11-14].

In a Lévy walk, agents show power-law distributed step lengths (l), as described by the following equation:

$$P(l) \sim l^{-\mu}, \quad 1<\mu<3$$

resulting in long-range exploration and effective searching for agents, when available food is scarce or food locations are far from their current positions [1-7, 9, 10, 17 and 56]. Many researchers focus on whether actual animals follow a Lévy walk, because foragers obeying this movement can survive for a long period without extinction.

Isolated desert ants are known to show Brownian or composite Brownian walking [19, 22, 57 and 58]. We conducted experiments using Japanese carpenter ants and examined the possibility of emergence of Lévy-like movements while swarming as compared with isolated foraging. We also conducted simulation analysis, examining whether power-law tailed properties could be achieved through interactions between Brownian walkers. We developed a random walk model that

occasionally produces long step lengths by considering the thickness of metric spaces. Agents in our model change directional rules by anticipating other local agents' moving directions. Thus, agents can increase the probability of directly going to location-bounded food. However, agents in our model are random walkers. Therefore, they do not know what profitable locations they can reach merely by obeying others' information. Consequently, we introduced a modulation effect in which agents modulate changed rule intervals depending on the number of other local agents. Agents would be able to produce internal noise, i.e. deviations in unknown goals, by increasing the probability of moving in specific directions. In this paper, we examine how this internal noise could contribute to obtaining power-law tailed step lengths.

2-4-2. MATERIALS & METHODS

EXPERIMENTAL MATERIALS

We used Japanese carpenter Ants, *Camponotus japonicus*, which are known to use tandem running rather than chemical pheromones, for recruitment. We collected 40 workers from Kobe University and housed them in a plastic box (62.5 × 43.5 × 32.0 cm high) into which a smaller plastic box covered by a red plastic sheet was introduced for their nest. Honeydew solutions were provided regularly, and fresh water was always available. We applied talcum powder on the walls to prevent workers from escaping. The colony was maintained at room temperature (21 ± 2°C) and regularly moistened.

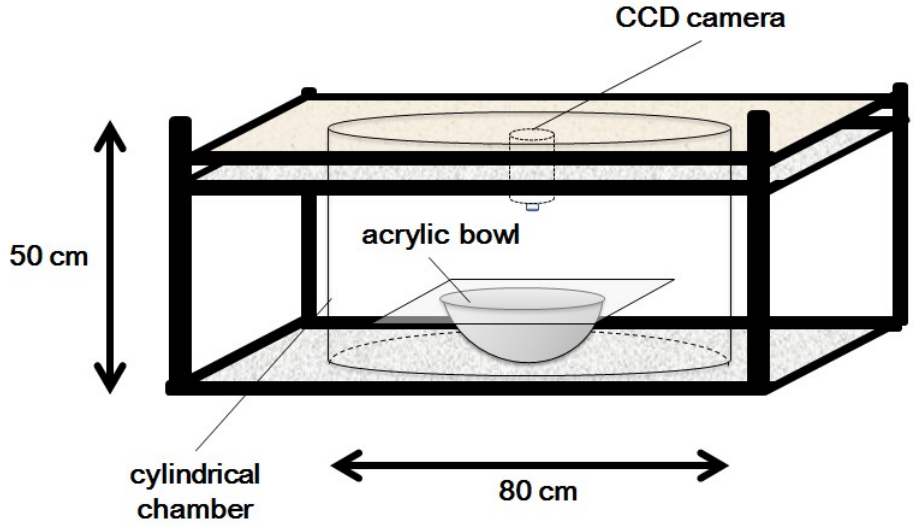

Figure 1. Experimental set up. An acrylic bowl serving as a test field is introduced into the experimental chamber, which is supported by frames. The experimental chamber is equipped to prevent visual surroundings from influencing ants' behaviours.

EXPERIMENTAL METHODS

A cylindrical chamber (80 cm in diameter, 57 cm high) was set in a square-shaped frame support (Figure 1). The chamber was covered with a wooden lid (90 × 90 cm). Three LED light bulbs (LDA6D-H-E17, 6.1 W) were symmetrically set on the inside of the cover having a hole at its centre through which a camera (HDC-TM700, Panasonic) could be inserted. An acrylic bowl (27.00 cm diameter) was introduced in the middle of chamber to be used as a test field. We set two test conditions: a swarm condition in which ten agents were placed together into the acrylic bowl and a single condition in which only a single agent was placed into the acrylic bowl. One trial was conducted under the swarm condition, and three were conducted under the single condition, because it was difficult to obtain trajectories of agents under the swarm condition during which agents occasionally overlapped. In order to evaluate step length distribution using Akaike weights, the number of data points should be more than twenty or thirty. Consequently, we were able to obtain not trajectories of all of the agents but four ants' trajectories from the swarm condition [34]. To match the number of data under both conditions, three ants' trajectories were obtained from control experiments by conducting three trials. Each trial lasted for one hour under both conditions. We obtained trajectories of the agents using image-processing software (Library Move-tr/2D ver. 8.31; Library Co. Ltd., Tokyo, Japan) set to one frame/sec. Each worker was used only once in our experiments, and the acrylic bowl was cleaned after each trial using ethanol solutions.

RULE CHANGE WITH INTERACTION (RCWI) MODEL

We randomly placed ten agents on a one-dimensional field (50 length field size with periodic boundaries. Each agent moved on the field by one length at each time step. We calculated 3,600 time steps as one trial. Each agent's movement began as Brownian motion. Therefore, the two intervals were initially set to

$$I_{0,k}(0) = [0.00, 0.50],\ I_{1,k}(0) = [0.50, 1.00]$$

for all k agents. The next walk is defined by the following equations:

$$\begin{aligned} x_k(t+1) &= x_k(t) - 1, \text{ if } R_k(t) \in I_{0,k}(t) \\ &= x_k(t) + 1, \text{ if } R_k(t) \in I_{1,k}(t), \end{aligned}$$

where $R_k(t)$ specifies a random number ($0.00 \leq R_k(t) \leq 1.00$) at time t.
If agents detect other agents within their own visual detection fields (2.00 radius), they change the directional rule as follows:

$$I_{0,k}(t) = [0.0, N_{0,k}(t)],$$

$$I_{1,k}(t) = [N_{0,k}(t), N_{0,k}(t) + N_{1,k}(t)],$$

where $N_{i,k}(t)$, $i = 0, 1$ is defined by

$$N_{i,\mathrm{k}}(t) = n_{i,\mathrm{k}}(t) / \sum_{j=0}^{1} n_{j,k}(t)$$

Here, $n_{i,\mathrm{k}}(t)$ is the sum of the following two values:

$n_{i,\mathrm{k}}(t) = base$ + (number of agents that are going to move *) = $base + sum(*)$
$* = -x(i=0), + x(i = 1)$

If $threshold_k \leq$ (Total number of agents detected by k^{th} agent),
then
$base = 0.01$
else
$base = 1.00$

We introduce the following values for all agents:

$$threshold_k \in \{1, 2, 3\}$$

Therefore, agents modulate the rule interval deviations on the basis of the number of other agents locally detected by changing the *base* from 1.00 to 0.01. Refer to Figure 2 for a flowchart of our model. Later, we discuss the reason for defining the detection field as 2.00 radii.

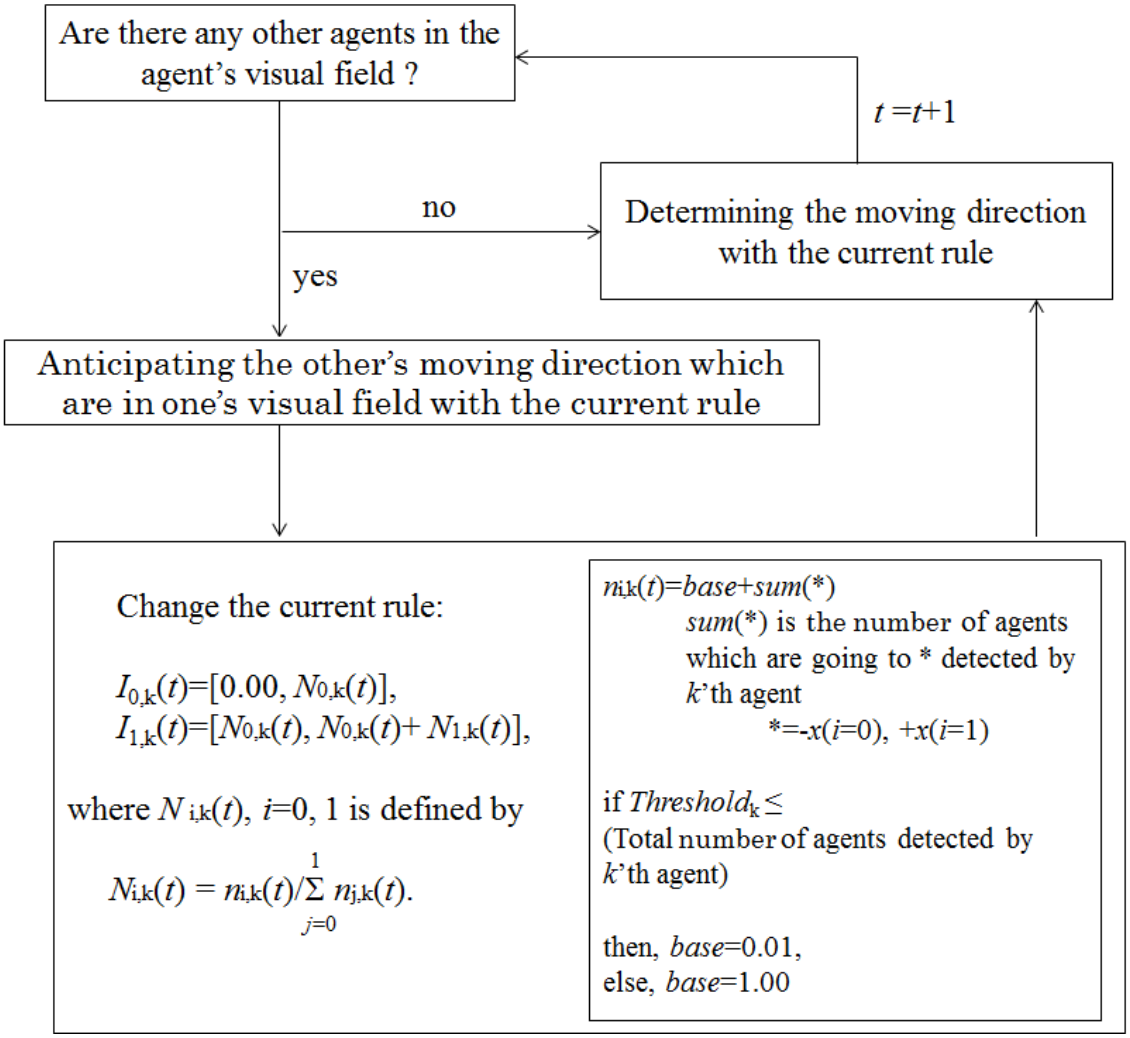

Figure 2. Flowchart of RCWI model. $I_{0,k}$, $I_{1,k}$ are directional rules for the k^{th} agent and initially set to $I_{0,k}$ = [0.00, 0.50], $I_{1,k}$ = [0.50, 1.00] for all agents. $n_{i,k}$ is the sum of two values: *base* and *sum*(*) . *sum*(*) is the total number of agents that are going to * detected by the k^{th} agent. * is–x if i = 0 and +x if i = 1. The *base* is set to 1.00 for all agents initially. Depending on $Threshold_k$, the *base* is changed to 0.01. $Threshold_k$ is assigned randomly to every agent for k = 1, 2 and 3. Please refer to the text also.

2-4-3. RESULTS

EXPERIMENTAL RESULT

First, we show our experimental results. Figure 3 shows an agent's trajectory obtained under the swarm condition. As seen in this figure, agents tend to rotate within the test field.

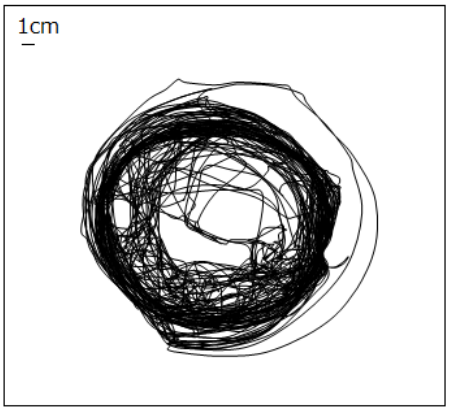

Figure 3. Experimental example of an agent's trajectory under the swarm condition.

Consequently, we defined a step length as the total length until both the x- and y-movement directions were changed, such as changing from clockwise to anticlockwise. Figure 4 illustrates step length results under both conditions. Combined data, i.e. stacking of several agents' data, were plotted here. In the swarm condition case, agents appear to show power-law tailed movements. In contrast, in the single condition case, they show exponential-tailed movements (Swarm: AIC weights of power-law = 1.00 against exponential-law (= 0.00), $\mu = 1.50$, n of data = 56, N of ants = 4, G-test: G-squared = 0.77, df = 3, $P = 0.86$, *NS*; Single: AIC weights of power-law = 0.00 against exponential-law (= 1.00), $\lambda = 0.0054$, n of data = 34, N of ants = 3, G-test: G-squared = 1.03, df = 3, $P = 0.79$, *NS*). We also evaluated what time property would emerge when the ants swarmed. Here, time durations for a single pair of agents were defined as they approached each other by 2.00 radii.

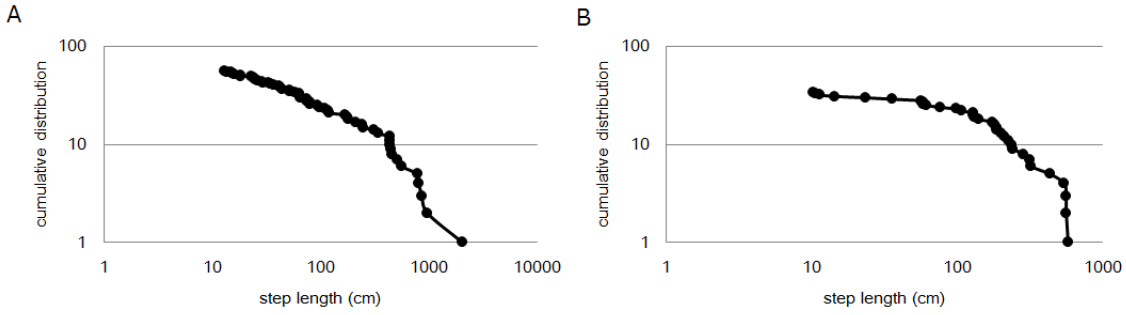

Figure 4. Log-log plots of experimental step lengths and cumulative distribution. A. Swarm condition (four ants). B. Single condition (three ants).

According to Figure 5A, an ant occasionally moves or stays together with a specific other agent for a long time as a result of power-distributed time durations (AIC weights of power-law = 1.00 against exponential-law (= 0.00), $\mu = 1.65$, n of data = 28, G-test: G-squared = 3.88, df = 3, $P = 0.27$, *NS*).

Furthermore, we checked the relation between time durations and migration lengths of one pair. Here, the definition of migration lengths was similar to that of step lengths. Each pair's displacements continue to increase until both the x and y movement directions of that pair are changed. If agents stay close to each other for a long time, the migration lengths of the pair of agents would become short displacements. However, if they actively move together, they travel longer distances. As shown in Figure 5B, there appears to be a weak linear relation between the displacements and time durations ($y = 0.11x + 2.09$, R-squared = 0.52). Consequently, they might move or stay together for specific durations.

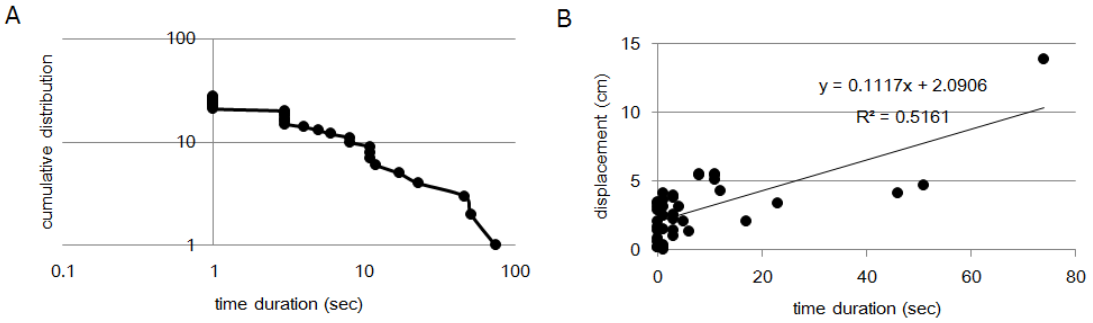

Figure 5. A. Log-log plots of experimental time duration and cumulative distribution. Time durations for a pair of agents are defined to ensure that they are no more than 2.00 cm apart. B. Relation between time duration and displacement of that pair.

MODEL RESULT

Second, we describe our simulation results. Figure 6 shows a single agent's trajectory from one trial. The agent moves straight and occasionally stands still while going back and forth. To evaluate the similarity between the experimental and simulation results, we defined step lengths as the total lengths until both the x and y movement directions are reversed. This definition is the same as the experimental definition. Similar to the experiments, agents in our simulation show power-law tailed movements, even though their initial movements were set to Brownian motion (Figure 7) (AIC weights of power-law = 1.00 against exponential-law (0.00), $\mu = 1.70$, n of data = 154, N of ants = 4, G-test: G-squared = 4.78, d$f = 3$, $P = 0.19$, NS). We also checked the time duration distributions of pairs of agents and the relation between time durations and migration lengths of pairs. The definition of migration lengths in our model was the same as that for the experiment. As shown in Figure 8A, similar results were obtained compared to those of the experiment. Though the relation between displacements and time durations varies depending on the pairs, pairs of agents appear to move or stay together for specific time durations (Figure 8A: AIC weights of power-law = 1.00 against exponential-law (0.00), $\mu = 1.47$, n of data = 54, G-test: G-squared = 4.54, d$f = 3$, $P = 0.21$, NS, Figure 8B: $y = 0.85x + 0.037$, R-squared = 0.94, Figure 8C: $y = 0.27x + 9.95$, R-squared = 0.31.

Figure 8C is the relation graph for the pair whose time distribution is shown in Figure 8A).

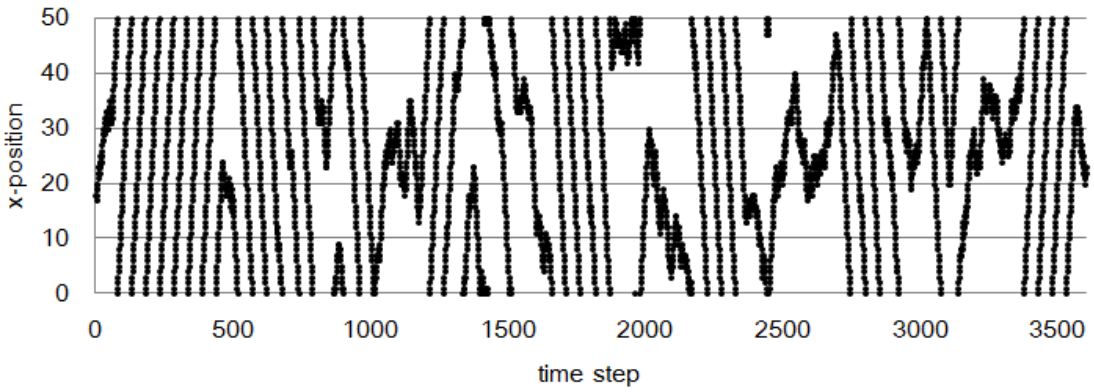

Figure 6. Simulation example of an agent's trajectory for one trial.

In both the experimental and simulation analyses, we defined the detection field as 2.00 radii. Figure S1 shows the relation between step lengths and cumulative distribution with respect to different detection field values (1.00 and 3.00 radii, respectively). If the detection field is set to 1.00, power-law tailed movement is achieved, but the slope value appears to be higher than both the experimental and default simulation values (Figure S1A: AIC weights of power-law = 1.00 against exponential-law (0.00), $\mu = 2.14$, n of data = 157, G-test: G-squared = 2.69, df = 5, $P = 0.75$, *NS*). If the detection field is set to 3.00, an unstable distribution appears to emerge (Figure S1B: AIC weights of power-law = 0.55 against exponential-law (0.45), $\mu = 1.66$, $\mu = 0.014$, n of data = 152). Consequently, we defined the detection field as 2.00 radii in our analysis.

Now, we show how modulation effects are important in obtaining results similar to the experimental results with respect to step length distributions. To this end, we set a fixed model as a control model in which no modulation effect exists. We set the *base* as 0.01 for all agents in this model. We conducted 11 trials for both models (RCWI model and fixed model) and evaluated the trial numbers that show power-law tailed rather than exponential distributions. There was a significant difference in the case of the RCWI model (Power-law distribution: ten out of 11 trials, binomial test: $P < 0.05$). However, in the fixed model case, both power-law tailed and exponential-tailed distributions were obtained equally (Power-law distribution: six out of 11 trials, binomial test: $P = 1.00$, *NS*). Consequently, we conclude that the modulation effect is crucial in achieving power-law distributed step lengths.

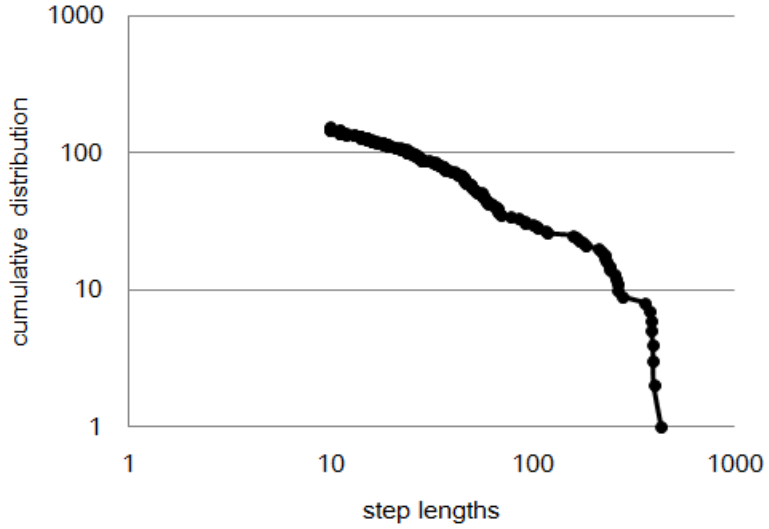

Figure 7. Log-log plots of simulation step lengths and cumulative distribution (four agents).

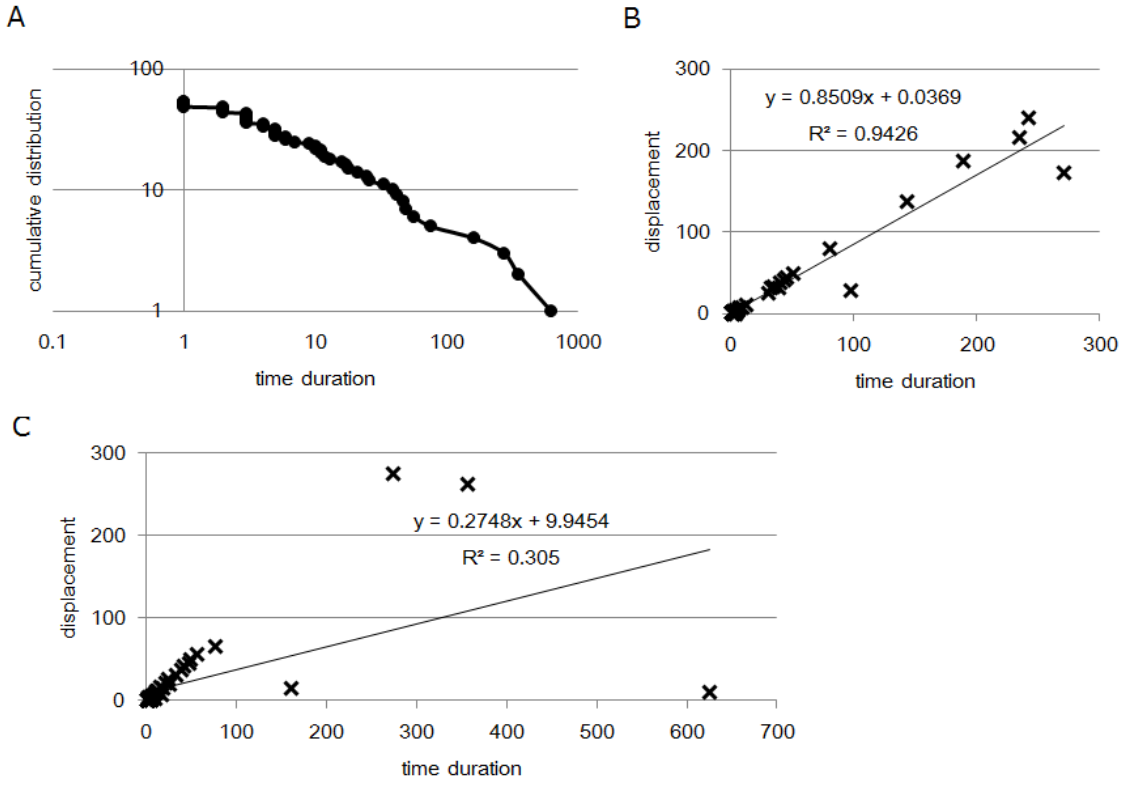

Figure 8. A. Log-log plots of simulation time duration and cumulative distribution. Time durations for pairs of agents are defined to ensure that they are no more than 2.00 cm apart. B, C. Examples of the relationship between time duration and displacement of each pair. The data used for the pair in C are used for it also in A.

2-4-4. DISCUSSION

We were able to observe Japanese carpenter ants showing Lévy-like movements when swarming, occasionally moving or staying together with other agents for a long time. These typical behaviours were observed also in our proposed multi-agent model. In our model, agents locally interact with each other by anticipating other agents' moving directions and changing their own directional rules. Agents appear to remain within small regions or move forward together with a specific agent while detecting the latter's movement and incorporating it back into their rules. In addition, deviations in changed rule intervals produced by modulation might occasionally be the key to achieving long step lengths, apparently contributing to obtaining power-law tailed walks in our simulation.

Desert ants are generally believed to follow Brownian-like walking [22, 57], occasionally showing composite Brownian walks, when searching their nest in unfamiliar environments [19, 58]. hey appear to follow a composite Brownian walk based on a composite correlated random walk mechanism and occasionally produce long-scale step lengths [59]. The composite correlated models could be the origin of Lévy walking. Recently, it has been reported that mussels follow Lévy-like movements, as composite correlated random walks, with a tri-exponential step length distribution [60, 61]. Their characteristic movements might be explained by mutual interactions as they detect two different population density scales, although the relation between a tri-exponential step length distribution and a two-difference scale model is obscure [34, 62].

Using a multi-agent model, we investigated how long-scale step lengths emerged through interactions. Agents identify a gap in limited surrounding spaces by modulating rule intervals, resulting in various-scale step lengths. Consequently, identifying different scale spaces would contribute to emergence of power-law distributions.

Agents relatively change their rules by simultaneously averaging others' moving directions by weighting the averaged directions relatively depending on the number of others. Therefore, they can occasionally follow specific agents for a long time. On the other hand, they move apart or stay in a limited number of regions for a while at other times. Interestingly, if we fixed the *base* to 0.01 (control model), we could not obtain reliable power-law tailed movements. This is perhaps because the ants might keep moving forward separately or together with others. In the control model, they appeared not to stay in restricted regions for a while, thereby missing wandering behaviour locally. These follower and parting behaviours might achieve a balance between resource exploitation and exploration.

Chapter 3

Logical Foraging and Visual Navigation in Foraging Ants

3-1 Visual learning and foraging in Japanese carpenter ants

3-1-1. BACKGROUND

Ant visual navigation is well studied and known to involve taxon-like processes, which orient foragers only in the forward direction and do not reveal so-called map-like navigation [63, 64 and 26]. Thus, the matched direction is always the direction in which to travel [65, 66]. Several studies have attempted to investigate the existence of mapping. However, it appears that ants cannot directly return home from far areas [54]. However, this inability does not exclude the possibility that ants cannot use map-like navigation. If an ant gives meaning, such as “accessibility” to landmarks or panoramic views, its relative location with respect to access locations may be achieved in the local area, indicating the use of local, map-like navigation. While oriented by taxon-like navigation, ant foragers must also simultaneously navigate by maps in local areas.

Here, using visual landmarks attached on the wall in test field, we investigated the possible existence of landmark meaning in ant navigation. As a result, we could obtain that Japanese Carpenter ants could attach meaning such as “accessibility” to landmarks and utilize them well. Moreover, they could use landmarks based on logical operations (AND / XOR). Therefore, we also investigated how agents solved the problem when logical contradictions arose.

3-1-2. MATERIALS & METHODS

We studied a Camponotus japonicus colony with 50 workers and a queen. The colonies were collected from Kobe University and housed in plastic foraging boxes (62.5 × 43.5 × 32.0 cm high). The wall of the foraging box was coated with talcum powder to prevent the ants from escaping. The foraging boxes were regularly moistened, and the colonies were maintained at room temperature (21 ±3°C). All experiments were conducted in an experimental chamber set in a frame. We fed the colonies two times per week with honeydew and once per week with mealworms. Fresh water was always available. Before the experiments, the colonies were starved for four to six days to ensure high foraging motivation.

EXPERIMENTAL APPARATUS

A cylindrical chamber (80 cm in diameter, 57 cm high) was set in a square-shaped frame support (Figure 1A, 2A). The chamber was covered with a wooden lid (90 × 90 cm). Three LED light bulbs

(LDA6D-H-E17, 6.1 W) were set symmetrically on the inside of the cover, and the center of the cover had a hole through which a camera (HDC-TM700, Panasonic) could be inserted. A circle hole (48 cm diameters, and 28.5 cm high) was installed in the chamber (Figure 1B, 2B). This hole was used as test filed. We introduced two different shaped landmarks into test field by attaching them on the wall. One is square landmark (9.5 × 7 cm) made from black copy paper. The other is circle landmark (3 cm diameters) made from black copy paper. These landmarks were attached to the wall from the ground at the distance of 2 cm. In each trial, the chamber was covered by the lid; thus, the only dominant visual cue was the equipped landmarks to test field wall. Acid-tracing paper was placed under the test field to prevent pheromone effects, and the paper was replaced before every test.

EXPERIMENTAL PROCEDURES

We defined 1 trial as the set of training phases and test phase for single agent.

AND/XOR CONDITIONS

TRAINING

We picked a forager from the colony and settled it on the center of test field gently. Each forager could move on field freely in training phase. Here, feeder or empty places were aluminum sheets (1 cm × 1 cm). A droplet of honey dew solution was put on the sheets in case of feeder places. No solutions were put on the sheets in case of empty places, on the other hand. In this condition, each agent was assigned to AND conditions or XOR conditions. No agent was used in both conditions.

In AND training phase, one feeder place and one empty place were introduced in front of a landmark. Each landmark (square or circle) were introduced to each agent randomly (See Figure 1C-i).The distance between feeder and empty places was approximately set as 9 cm. We defined agents' experiences of feeder or empty places as they attached the aluminum sheets physically within the angle observed through the CCD camera. We conducted training phases twice for single agent by switching feeder and empty places.

In XOR training phase, two feeder places were introduced in front of a landmark (square or circle) and the agent foraged freely. After consuming both honey dew solutions, two empty places were introduced in front of that landmark. Therefore, the agent experienced feeder sites (two feeder sites equipped to a landmark) and empty sites (two empty sites equipped to the same landmark) after that independently (Figure 1C-i).

TEST

Afterward, test phase followed.

In AND test phase (for agents trained in AND conditions), two empty places were introduced in

front of the same landmark used in training phase for that agent. It took approximately 30-40 minutes to conduct 1 trial for single agent (AND training – test). In XOR test phase (for agents trained in XOR conditions), two empty places were introduced in front of the same landmark used in training phase for that agent. It took approximately 30-40 minutes to conduct 1 trial for single agent (XOR training – test) (See Figure 1C-ii).

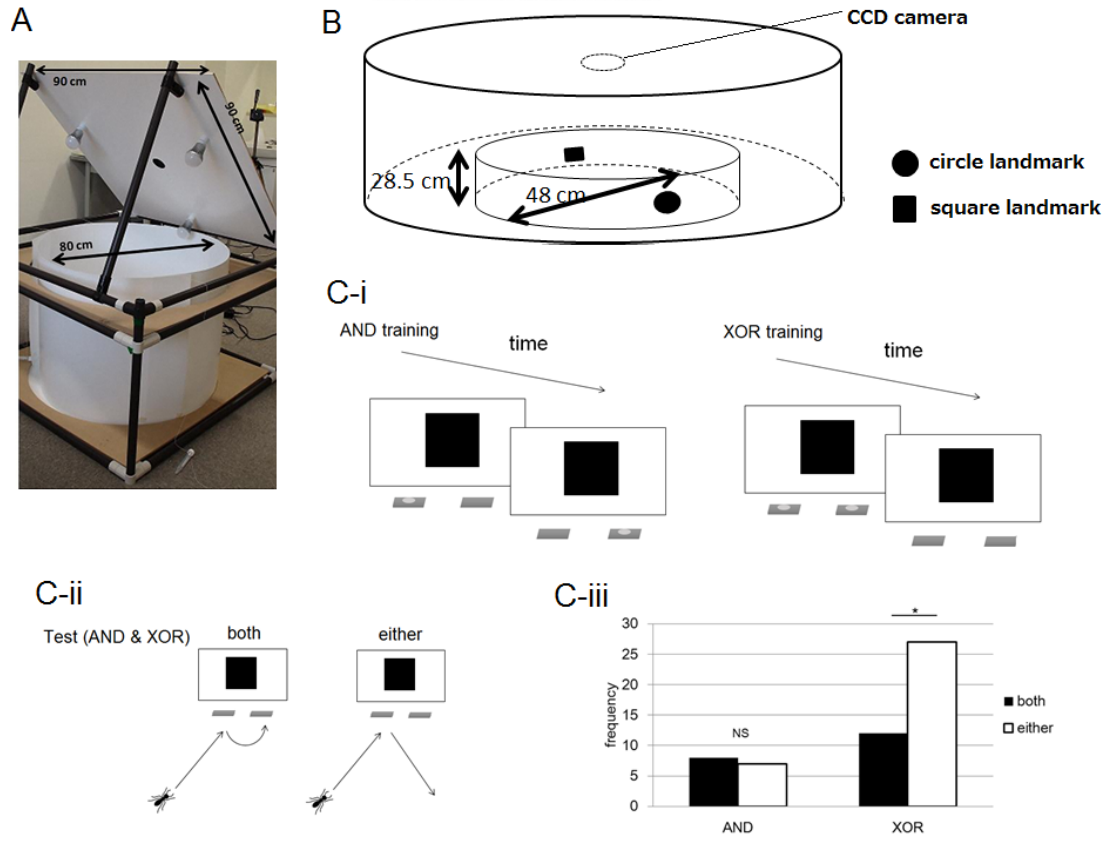

Figure 1. Experimental set up. A. The experimental chamber and a frame that supports the chamber. B. The schematic of experimental chamber and inserted test filed hole. C. The schematic of training or test. C-i. Training phase. C-ii. test phase. C-iii. Frequency of agents which showed each category (*both*/*either*). Grey squared figures indicate empty places and light grey dots indicate honey dew solutions (feeder sites).

GENERATION CONDITIONS

TRAINING

We picked a forager from the colony and settled it on the center of test field gently. Each forager could move on field freely in training phase. We stopped training when she experienced both feeder and empty places. Here, feeder or empty places were aluminum sheets (1 cm × 1 cm). A droplet of honey dew solution was put on the sheets in case of feeder places. No solutions were put on the sheets in case of empty places, on the other hand. In training phase, one feeder place and one empty

place were introduced in front of either each landmark at a distance of 4 cm respectively (See Figure 2C-i). We defined agents' experiences of feeder or empty places as they attached the aluminum sheets physically within the angle observed through the CCD camera. We conducted training phases twice for single agent.

TEST

Afterward, test phase followed. We conducted two test conditions. One is generation condition in which both landmarks (square and circle) were set on side by side as one landmark. Two empty places were introduced in front of both landmarks (See Figure 2C-ii). The other condition is named control condition in which landmarks were set on separately as same as that of training phases excepting that two aluminum sheets were introduced in front of each landmark as empty places (See Figure 2C-iii). In test phases, two aluminum sheets were lined side by side at a distance of approximately 9 cm in front of the landmark and no feeder places were used in both conditions. It took approximately 30-40 minutes to conduct 1 trial for single agent (two training phases and one test phase (either generation condition or control condition). The combination of landmarks (square or circle)×places (feeder or empty)×test condition (generation or control) were chosen randomly on each trial.

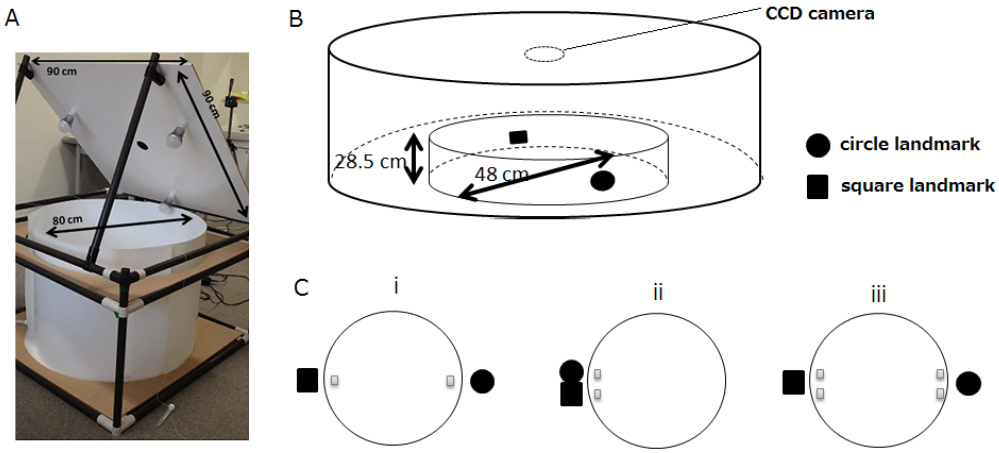

Figure 2. Experimental set up. A. The experimental chamber and a frame that supports the chamber. B. The schematic of experimental chamber and inserted test filed hole. C. The schematic of training or test situations from top view of test field. C-i. Training phase. C-ii. Generation condition of test phase. C-iii. Control condition of test phase. Grey squared figures indicate the feeder or empty places.

3-1-3. RESULTS

AND/XOR CONDITIONS

Figure 1C-iii indicates the frequency of experiences of *both*/*either* empty place(s). In case of *both*

situation, ants experiences both empty places lined side by side without more than 90° turns. In case of *either* situation, ants show more than 90° turn after experiences of either empty place lined side by side. It appears that no significant differences were found in this condition (binomial test, both: 7 out of 13, P=1.00, NS). Contrary to that, agents appeared to go to only one site in case of XOR conditions. Thus, significant differences were found (binomial test, both: 11 out of 39, P<0.05). It appears that agent could attach the meaning to landmarks and logically learnt them.

GENERATION CONDITION

First, we examined ants could learn feeder or empty locations in connection with the visual landmarks separately. Here we checked how many numbers of experiences were counted in response to the number of visit to calculation regions. We defined the calculation regions as the square regions (13 × 9 cm) between two aluminum sheets (Figure 3A). Ants sometimes come in this region to find feeder. It is reported that ants can detect two landmarks as different ones in case of they are close to the landmarks. Therefore, it is expected that they reach this region occasionally in our test phases. If they can detect the differences between two landmarks visually, they would turn or escape from the region without experiences of empty places in case of making for empty landmark. Contrary to that, in case of making for feeder landmark they would stay or search within that region with experiences of empty places. Figure 3B indicates the mean percentage of experiences of empty places against total number of visit to calculation regions. It seems that ants can detect the differences between two separate landmarks visually and learn feeder or empty places in connection with visual shapes (Welch Two Sample t-test, $t = 2.77$, $df = 5.469$, $P<0.05$).

Figure 4 indicates the frequency of experiences of both/either empty place(s). In case of *both* situation, ants experiences both empty places lined side by side without more than 90° turns. In case of *either* situation, ants show more than 90° turn after experiences of either empty place lined side by side. In follower case therefore, ants would go away from the landmark after checking only one aluminum sheet. According to Figure 4, ants would go to both empty places consecutively if two landmarks were lined (generation condition) (generation condition: binomial test, both: 5 out of 13, $P=0.58$, NS, control condition: binomial test, both 0 out of 10, $P<0.01$, generation vs. control: fisher's exact test, $P<0.05$). We discuss the significance of our results in next session.

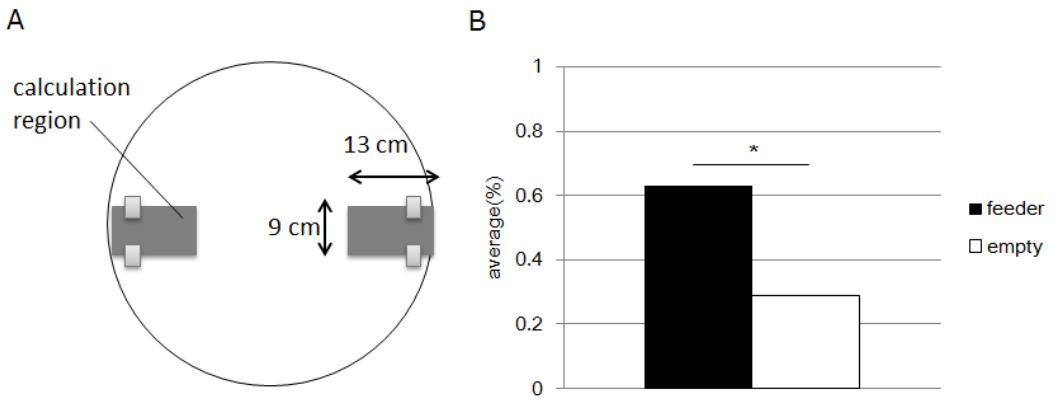

Figure 3. A. Schematic of calculation region indicated by deep grey squares. Small grey square figures indicate empty places. B. Average-percentage of experiences. Feeder indicates the landmark which agents learned they could find feeder in front of that landmark. Empty indicates opposite landmark for feeder landmark.

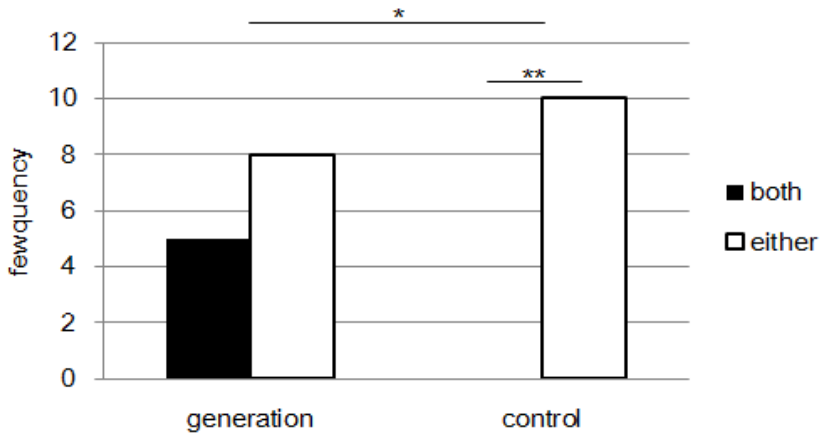

Figure4. Frequency of empty places-experiences in respect to *both* and *either* situations. $^{**}P<0.01$, $^{*}P<0.05$.

3-1-4. DISCUSSION

Our results indicate that ants can learn visual landmarks by associating to accessibility from that stimulus. Therefore, perhaps, they can attach meaning to each landmark. Moreover, they change their behaviors based on logical foraging (AND/XOR). However, using different levels of navigation mechanisms (meaning and landmark itself) would result in contradictions occurred. To overcome these problems, they might manipulate different two landmarks as novel one. Our LM generation test suggests those results. Therefore, when experimenters observe these results, they may come to the conclusion that simple error occurs. However, our results indicate the possibility of internal noise produced by each agent. Agents might confuse different levels of navigation mechanisms, which

results in producing novel landmarks. These behaviors would contribute to achieve the balance between exploitation and exploration for visual navigations.

Chapter 4

Kanizsa Triangle Illusion: Weak Cognition

4-1 Human perception formed and destroyed by local obstacles or foraging ants

4-1-1. BACKGROUND

Regarding to perceptions, it's well discussed whether animals, including human, perceive the whole pictures or just element part level [67-70]. However, in any case, it seems that there is a tendency to make judgment which level is true or not, in assuming that each level is independent of each other. Some studies reported that experimental subjects' persistency to either level is changeable depending on situation contexts. [71]. Therefore, there is plenty of space to consider new mechanism to explain of above flexible decisions i.e. employing local element information with referring global property.

Kanizsa triangle figure, in which three Pac-Man are directed inside symmetrically, is well known as illusion that subjective contour is perceived although such contour never exists actually and well referred as good example of gestalt perception [72, 73]. In the transcendence perspectives, the apparent triangle appears as a perceptive object based on perceptual processing in visual cortex. Gaetano Kanizsa reported in his own work that these subjective contours might appear from imperfective property which element of this contour (each Pac-man) had [73]. He said that because we had such intrinsic tendency, contour would be formed as prospect objects which could fill the chipped actual objects.

What it is like to perceive the subjective contour which is actual non-existence? Can we explain this without assuming transcendence perspectives?

We assume that perceiving the functional whole as a result which attributes to implication of elements is illusion perception. In other words, we assume that Kanizsa triangle illusion aroused from the two different levels' interaction of part i.e. each Pac-Man in visual field. Each Pac-Man exists as an object on one hand. On the other hand, however, the global property or meaning of those inducers must be referred as different level. Therefore, introducing the stripe notches which indicate another possibility of parts' global property or meaning, subjective ambiguous might be produced and affect the reliable establishment of contours. Actually, it is reported the possibility of gestalt grouping in unconsciousness [74]. We discuss consistency of our assumption by introducing the perception difference of subjective contour between two visual stimuli which have same imperfective property and tackle to the origin of Kanizsa triangle illusion.

In our working hypothesis, apparent pattern is produced spatially accelerated or inhibited, dependent on a local pattern which serves as bias. We here argue the relationship between the imperfective property mentioned by Kaniza and pattern formation in a bottom up fashion. Especially,

we introduced Kanizsa triangle figures equipped with some stripe notches to experimental subjects.

To evaluate how much these notches affected establishing relevant clear contour, we investigated whether notches' inserted positions or directions affected contour establishment or not. If implication of inducers (Pac-man) has something ambiguous directional information, positions or directions of stripe notches influence expectation based on local information i.e. inducers. Later, we discuss the consistency between our obtained results and above mentioned assumption. In addition to human experiments, we also conducted investigation whether garden ant *Lasius. niger* drives whole perception (kanizsa triangle illusion) or not. Here, exposing ant *Lasius. niger* colony to kanizsa triangle figure made of honeydew solutions, we discussed origin of this illusion occurrence as whole from part, excluding transcendence perspectives. In ant studies, it is suggested that various interactions of agent levels effect colony decision-making [24, 75]. Ant foragers can consume additional food even after consuming a certain amount of food [76]. So it is not strange to discuss foragers' moving trajectories between some food regions i.e. Pac-Man shaped food sources.

4-1-2. MATERIALS & METHODS (Human experiments)

Stimulus materials

We made five special Kanizsa triangles. These five figures were named vertical, horizontal (edge), slant, top and hollow, respectively (Figure 1).

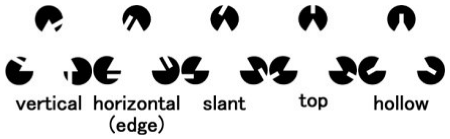

Figure 1. Five special kanizsa triangles.

The diameter of the circles which form triangles were 3.4mm. The distance between any two inducers was 6.8mm. The width of the stripe notches (white bars) were 0.4mm.

After that, We selected two figures from five figures, and made four combinations (Figure 2).

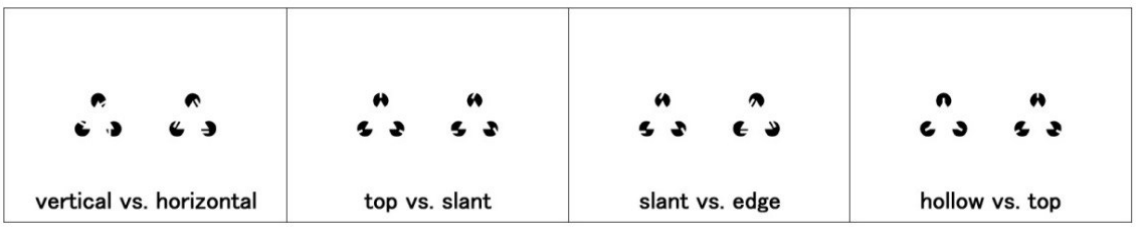

Figure 2. Four combinations.

Here, we made mirrored figures of vertical, horizontal(edge) and slant respectively (Figure 3).

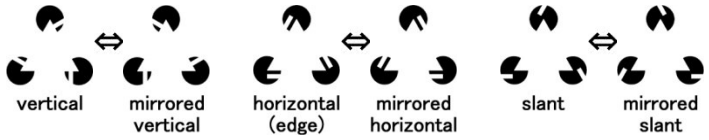

Figure 3. Mirrored figures.

The reason why we made mirrored figures is to check whether there are differences about vision between original triangles and mirrored triangles. Mirrored triangles also made some combinations.

Thus, we had total twelve combinations including mirrored combinations. For example, there are four combinations which are related to vertical and horizontal.

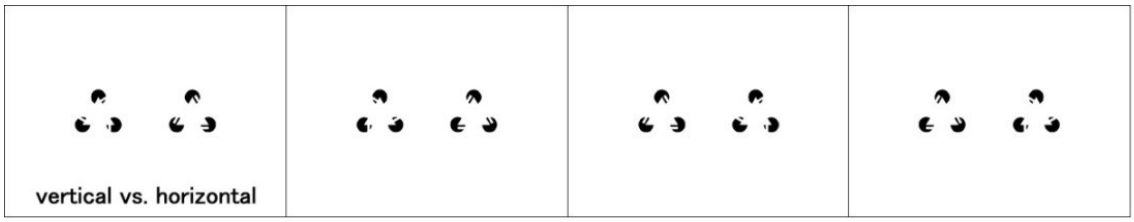

Figure 4. Four combinations related to *vertical* and *horizontal*.

In addition, we prepared four simple Kanizsa triangles (Figure 5).

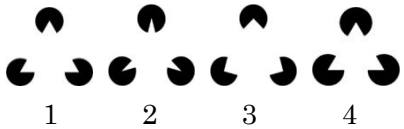

Figure 5. Four simple Kanizsa triangles.

We also selected two figures from four figures, and made eight combinations excepting 2-4, 4-2, 3-4, 4-3 configurations. So, we have total twenty combinations. We printed those twenty figures individually on the twenty high-quality cards which were postcard-sized.

Procedure

Participants were fourteen university students. First, they were instructed about procedure of this experiment. After that, they were shown normal Kanizsa triangles and asked whether illusory figures could be seen. If a participant could not see illusion at this stage, then we excluded his or her data. Second, participants were given the twenty cards which were explained above. In addition, they were given the question and answer sheets. Those sheets had two questions per one combination of figures. And two questions were same in all twenty combinations.

Participants turned the twenty cards one by one and answered the questions. Eight combinations of

the simple Kanizsa triangles were printed on first eight cards, and twelve combinations of the special Kanizsa triangles followed those. It is because we thought it was very hard for participants to answer the questions about the special Kanizsa triangles without preparations. So we prepared the eight exercises using the simple Kanizsa triangles.

By the way, participants had to have intervals of two seconds between twenty tests to rest their eyes and brains.

Questions

1 st question: intentisity

The first question which was asked about combinations of figures was 'Which figure has the more clear outline of the triangle?' To answer this question, participants were given the following four choices.

1. The left figure has the more clear outline.
2. The right figure has the more clear outline.
3. Both figures have clear outlines. (I can't choose one.)
4. Both figures don't have outlines.

2 nd question: deformation

The second question was 'Do you see a triangle which outline is distorted?' To answer this question, participants were given the four choices again.

1. The left figure has the more distorted triangle.
2. The right figure has the more distorted triangle.
3. Both figures have a distorted triangle. (I can't choose one.)
4. Both figures don't have a distorted triangle.

From the above, the flow of the experiment was following.

1. We instruct about procedure of this experiment.
2. Participants are shown normal Kanizsa triangles and are checked whether they have competence to participate in our experiment.
3. Competent participants are given the twenty cards and the question and answer sheets.
4. Participants turn the card one by one answering the two questions at their own pace, but they have to have two seconds intervals between tests.
5. When the twentieth card is turned and participants finish answering the two questions, this

experiment is finished.

4-1-3. RESULTS (Human experiments)

We formed the results of the above experiment into the four groups. The four groups correspond to four combinations of Figure 2. In the combinations of vertical and horizontal, the vertical, horizontal and both rates for the first question were almost same. (Fisher's.test : vertical 19 out of 54, horizontal 17 out of 54 and both 18 out of 54, p=0.946, Figure 6-1.) The neither rate for the second question was reasonably high. (Fisher's.test : vertical 1 out of 56, both 1 out of 56 and neither 54 out of 56, p<0.001, Figure 6-2.)

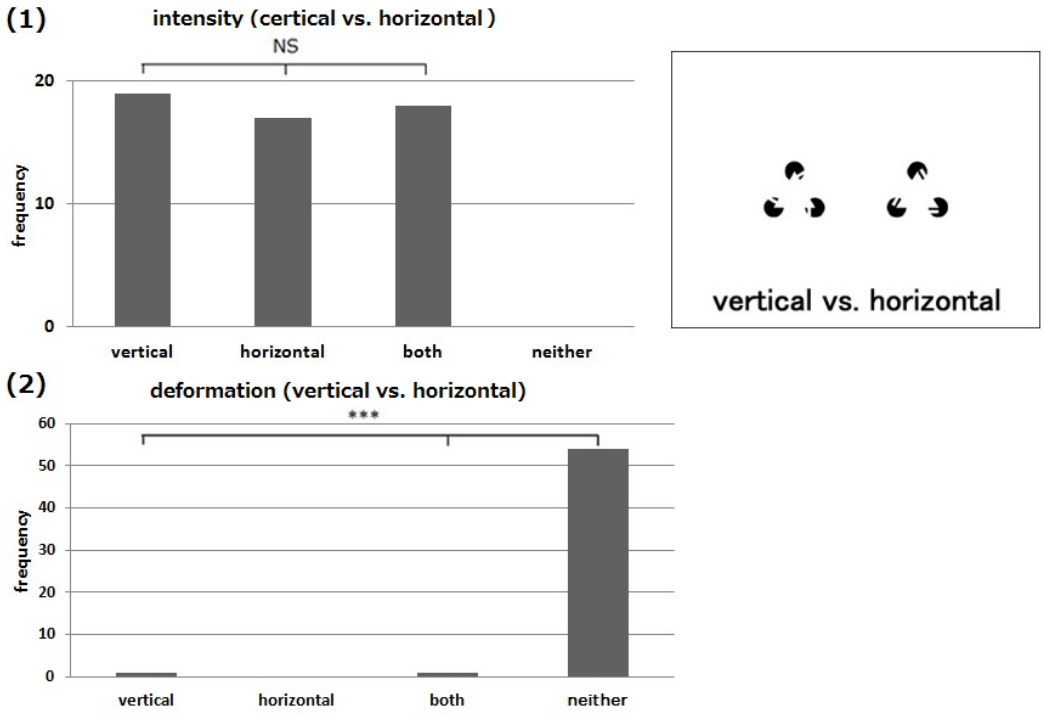

Figure 6. Experimental results of vertical vs. horizontal (1). intensity. (2) deformation

In the combinations of top and slant, the top, slant and both rates for the first question were divided (Fisher's.test : top 9 out of 28, slant 5 out of 28 and both 14 out of 28, p=0.1132, Figure 7-1).
The neither rate for the second question was reasonably high (binomial.test: slant 1 out of 28 and neither 27 out of 28, p<0.001, Figure 7-2).

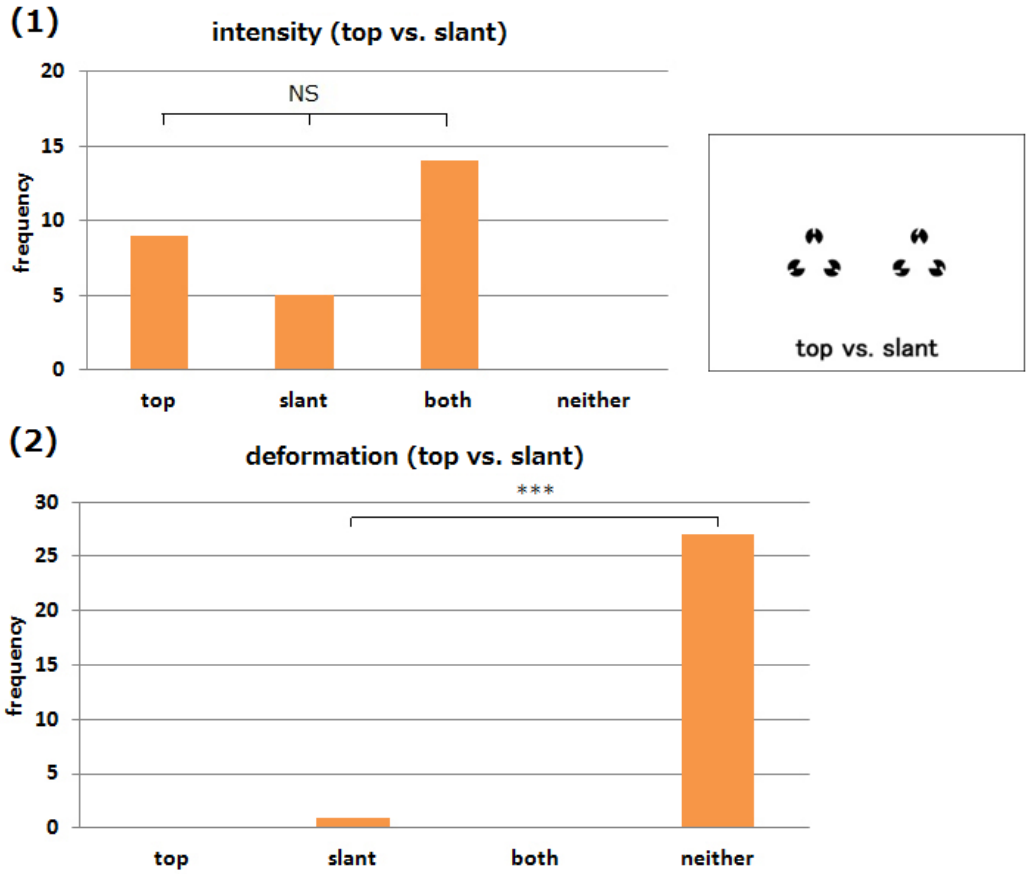

Figure 7. Experimental results of top vs. slant. (1). intensity. (2) deformation

In the combinations of slant and edge, participants selected the slant at a high rate in the first question (Fisher's.test : slant 38 out of 56, edge 6 out of 56 and both 12 out of 56, $p<0.001$, Figure 8-1).

The neither rate for the second question was reasonably high (Fisher's.test : edge 1 out of 56, both 1 out of 56 and neither 54 out of 56, $p<0.001$, Figure 8-2).

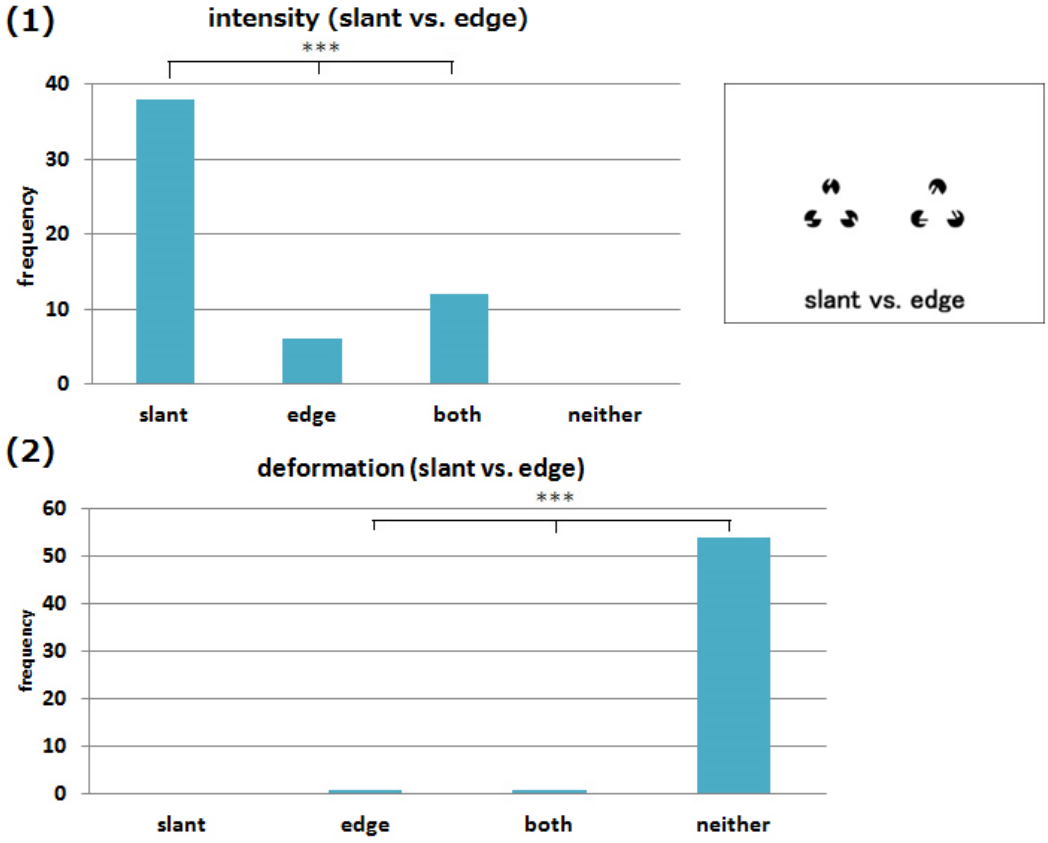

Figure 8. Experimental results of slant vs. edge. (1). intensity. (2) deformation.

In the combinations of hollow and top condition, participants selected the top at a high rate in the first question (binomial.test: top 25 out of 29 and both 4 out of 29, $p<0.001$, Figure 9-1).
And, participants selected the hollow at a high rate in the second question (binomial.test: hollow 20 out of 28 and neither 8 out of 28, $p<0.001$, Figure 9-2).

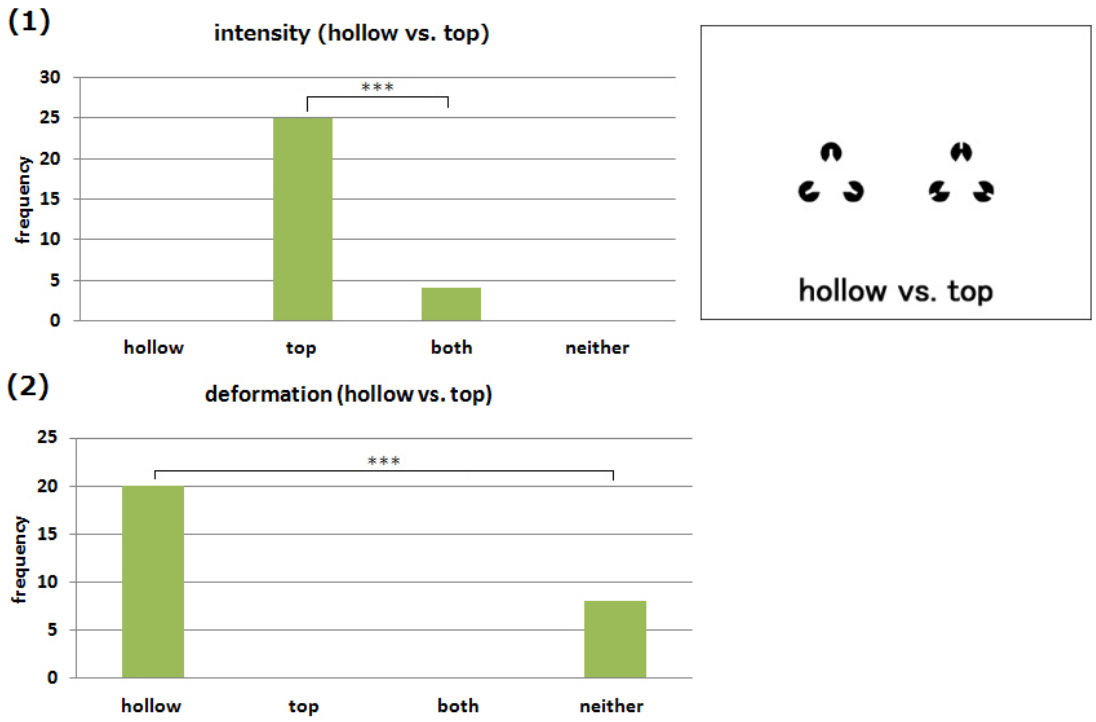

Figure 9. Experimental results of hollow vs. top. (1). intensity. (2) deformation.

Finally, we checked whether there is consistency in the individual participant's answers among four combinations related to vertical and horizontal (See Figure 4).

The result is the Figure 10, and consistency was very high (binomial.test: consistency 43 out of 56 and inconsistency 7 out of 56, $p<0.001$).

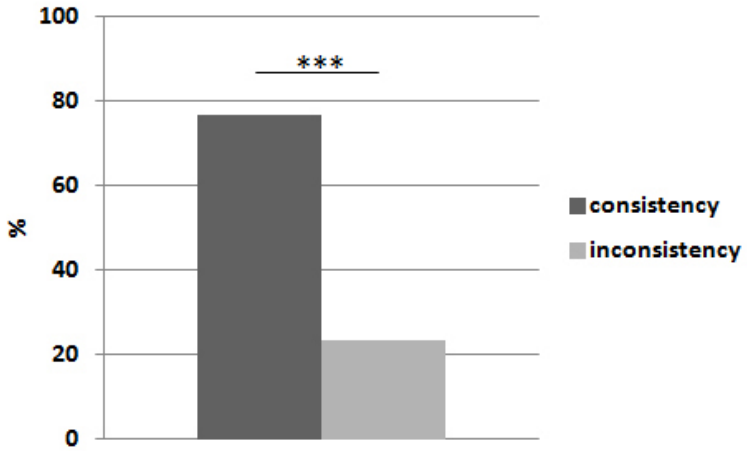

Figure.10. Consistency of individual participant's answers in vertical vs. horizontal

4-1-4. MATERAILS & METHODS (Ant experiments)

Rearing conditions

We studied a *Lasius niger* queen-less colony with 500-600 workers. This colony was collected on the Kobe University and housed in plastic foraging boxes (35.1 × 25.5 × 6.1 cm in height). This box contained a plastic nest-box (5.1 × 5.5 × 1.1 cm in height) covered with clear red plastic sheets. The wall of the foraging box was coated with talcum powder to prevent the ants from escaping. All experiments were conducted in a room (26.1±C) with artificial room light. We fed the colony two times per week with honeydew and once per week with mealworms. Fresh water was always given. Before the experiments, the colony was starved for four-five days to ensure high ants swarm.

Experimental set-up

We made kanizsa triangle shaped food with honeydew solution (50% w/w) on cardboard by brush-painting. We hollowed out OHP sheets in the form of kanizsa triangle figure and laid cardboards under that in order to paint honeydew. The figure consists of three Pac-Man disposed symmetrically whose diameter were 1.4 cm. The distance between the centres of a Pac-Man was 4.0 cm. Then, subjective contour's side lines were set to 4.0 cm long (Figure 11-1). We set control experiments using three dots figure instead of Kanizsa triangle figure. Each dot consisting of three dots figure had 1.4 cm diameter and disposed in the same way as kanizsa triangle figure (Figure 11-2).

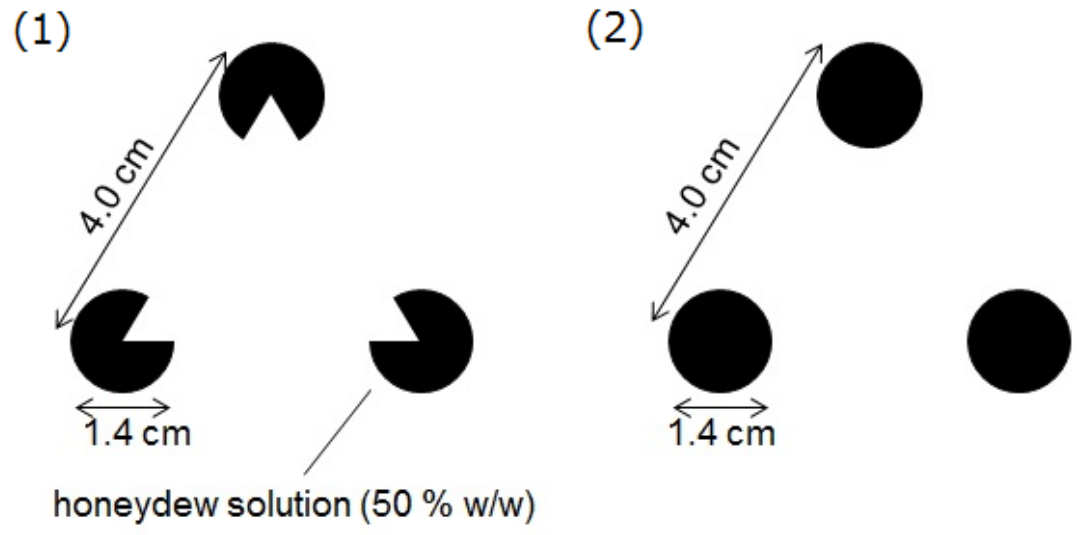

Figure 11. Schematic examples of experimental stimulus. (1). Kanizsa trialnge illusion figure. (2). Figure for control experiments.

The cardboard, on which a honeydew kanizsa triangle or three dots figure was painted, was installed

in a plastic foraging box. Swarm patterns of agents were recorded with video camera (SONY). For each version (Kanizsa triangle version, control -three dots- version), only one trial was conducted on each experimental day. One trial took approximately 10-20 minutes. The trial sequences (1st kanizsa and 2nd control or 1st control and 2nd kanizsa) were conducted evenly. Four trials were conducted for each version. To track ant trajectories and obtain x-y coordinate (5 frames per second), we used image-processing software (ImageJ: Rasband WS, National Institutes of Health, Bethesda, Maryland, USA). The density of the ants was then calculated (R, version 2.15.0). To smooth the analysis and eliminate unnecessary dense peak, unchanged x-y values through one frame to next were excluded from analysis.

4-1-5. RESULTS (Ant experiments)

Analysis

We set the analysis area in the range which had 2.45 cm long and 1.68 cm wide from an intersection point of perpendicular lines (light grey zone in Figure 12-1). Then, we calculated the mean position (bold line in light grey zone in Figure 12-1) by setting the calculate area (deep grey zone above light grey zone in Figure 12-1) which was defined as dense regions above threshold dense (> 60 %).

These mean positions were obtained every 0.025 cm. We excluded honeydew regions because these areas were too dense to detect ants' moving trajectories (Figure 13 and 14).

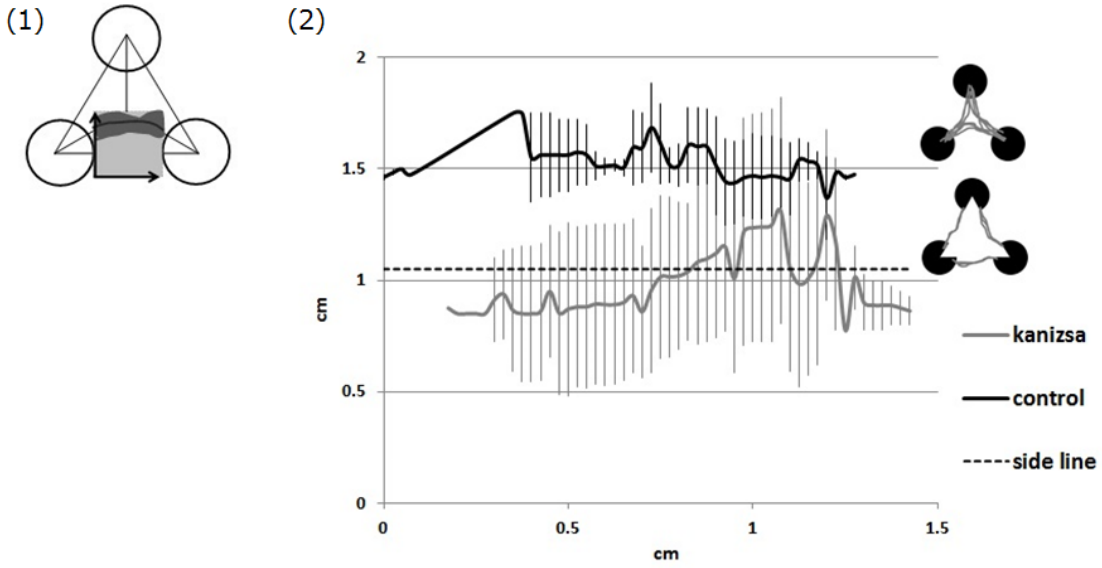

Figure 12. Average position of agents' trajectories. (1). Schematic figure of analysis. Light grey indicates calculation areas. Dark grey region indicates detected densities. Grey bold line indicates average position of detected densities. Bold vertical arrow indicates Y-axis and horizontal line indicates X-axis respectively. (2). Average position with respect to swarm trajectories.

Experimental results

Considering honeydew arrangements, it is obvious that ants' dense peaks concentrate on the honeydew areas and form Pac-Man or dot shapes on each version respectively (Figure 13).

Figure 12(2) shows that dense mean positions on each version. In kanizsa triangle versions, the positions were lower than control versions' position and nearer to side line i.e. a side line between two vertexes, indicating that agents' moving directions biased to edge-point directions (kanizsa vs. control: Mann-Whitney U test: P<1.0E-15). Actually, the dense position peak near triangle centre regions was lower in kanizsa triangle versions than control's one in which ants' trajectories formed Y-shaped ones (Figure 14).

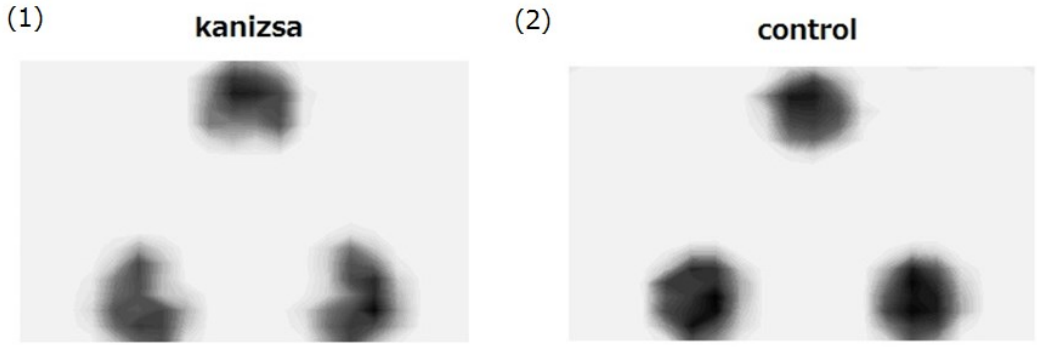

Figure 13. Example of swarm densities before peak positions removed. (1). Kanizsa version. (2). Control version.

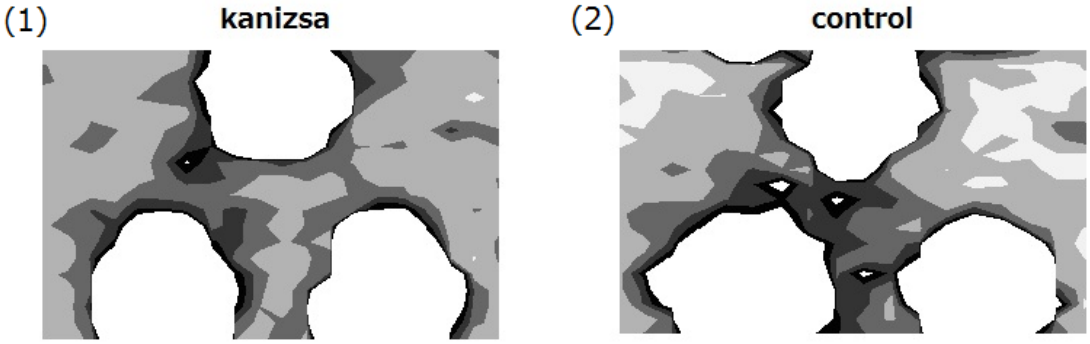

Figure 14. Example of swarm densities after peak positions were removed. Note that these figures were directly used to analysis. (1). Kanizsa version. (2). Control version.

4-1-6. DISCUSSION

Our results show that inserted notches position (whether these are added on top or edge of each Pac-man) influences subjective contours. It seems that if stripe notches are inserted on edge of inducers, perceived contour intensity is relatively less than that of slant versions. There was no

insistency difference between top and slant versions. In addition to that, hollow versions' perceived intensity is less than that of top versions.

Therefore, it might be possible that edge or inner part of inducers relatively contribute to contour perception compared with the Pac-Man with notches in outer part. These illusion figures which have relatively less contour intensity seem to crimp formation of relevant contour between any pair of inducers, perhaps because they let agents to find another possibility as a result of ambiguous exploration from local implicated information.

Our results suggest that local projecting part formed by concave triangle in the Pac-man could be spatially accelerated and connected with each other, which could produce contour perception. Notches near the projecting part (edge, hollow) could disturb producing subjective contour, compared with the Pac-Man with notches in outer part.

We found that there was no intensity difference between horizontal and vertical versions. It is unlikely that dominant eye effects influence that result because of our experimental conditions. Plus, we could obtain that individual perception had consistency regarding vertical and horizontal versions. Therefore, there must be higher-order cognitive processes about that. It's interesting that perceived intensity is different depending on the person. However, it's difficult for us to determine that reason and is needed more investigations.

Agents might perceive illusion contour as objects while finding or detecting new possibility and stimuli with active expectation which has been passively triggered by local information. Thus, balancing between activeness and passiveness would play an important role in illusion perception.

According to [77], Y-shaped trajectories formed in control versions might be obtained from random exploration after feeding on a food site, here, it was each honeydew dot [77]. Then, each honeydew dot appeared to be treated separately and independently. *Lasius.niger* foragers are well known to use chemical pheromones to recruit their nest mates [78, 79]. As a sequel to such random exploration and pheromone effects, Y-shaped dense peak was built. Contrary to the control versions, "subjective" contour was built in kanizsa triangle versions. Thus, whether or not there are edges formed by foragers would appear to contribute to foragers' moving directions. Ant's visual ability is limited. So they get information from limited local areas around them. From our experiments, it appears that edge of Pac-Man might give foragers directional biases and navigate them.

Regarding to occurrence of kanizsa illusions, it is possible that human subjects might produce some prediction and discover the predicted sources such like another edge of other Pac-Man. As a sequel to that consistency, subjective contour will be perceived. In this sense, it is possible that weakened contour is produced in case of inconsistency [80-82].

As considering diversity at micro-level, foragers might actively produce ambiguous information by local cues. Then, ambiguity and uncertainty may cause many explorative possibilities and play an essential role to flexible navigation and foraging [24, 52 and 53].

Appendix - Supporting materials

2-1 Emergence of optimal searching from Brownian walks

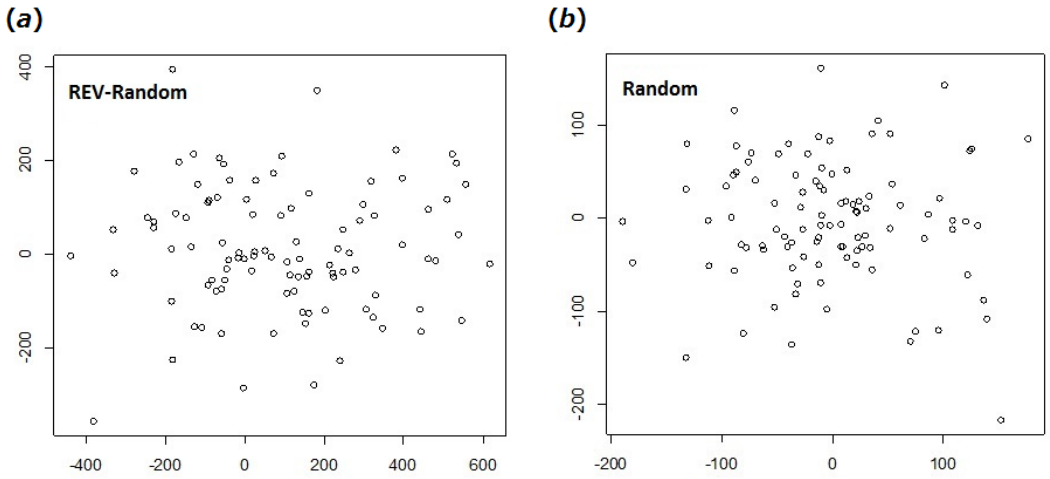

Figure S1. Distribution of end location along *x*-*y* coordinates after 10,000 steps (100 trials). (*a*). REV-Random. (*b*). Random.

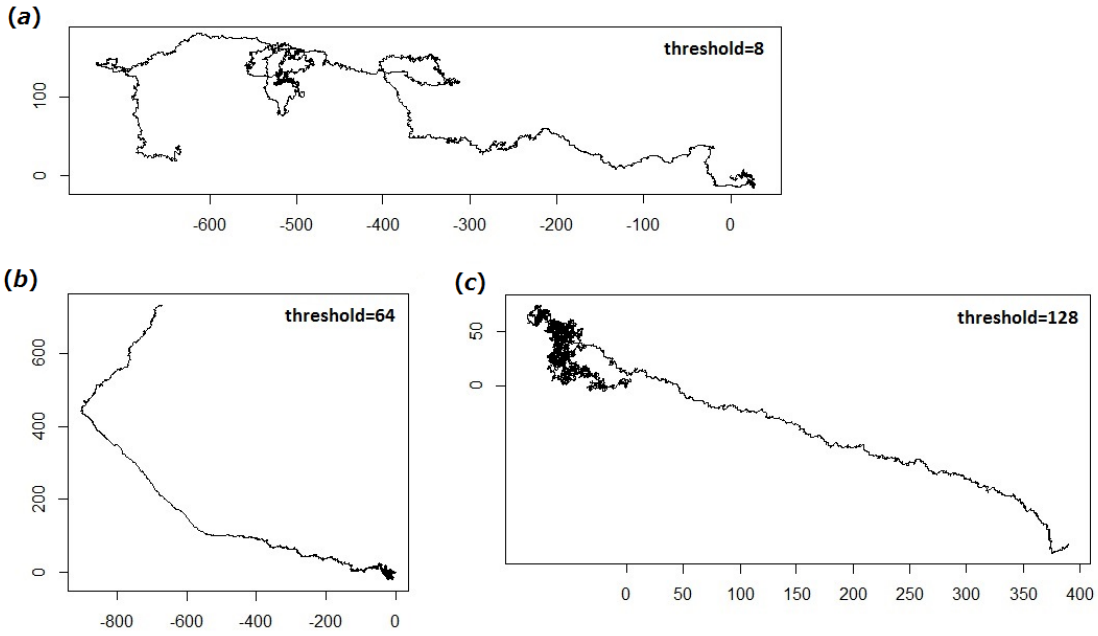

Figure S2. Example of agent trajectories over 10,000 time steps for various threshold values (θ) using the REV-Random algorithm. (*a*). Threshold value=8. (*b*). Threshold value=64. (*c*). Threshold value=128.

2-2 The relationship between "randomness" and "power-law" on Lévy-like foraging

	AIC of power-law weights $w(p)$	AIC of exponential-law weights $w(e)$	μ	λ	N
X	0.00	1.00	2.37	0.70	859
Y	1.00	0.00	2.76	0.97	844

Table S1. Results of AIC weights for each directional step lengths calculation from 1 trial in REV algorithm. Step lengths were defined as displacement between any consecutive trajectory points. We obtained trajectory points at 10 time step intervals. *N* indicates the number of trajectory points for each direction. If step length's value was 0, that value was excluded from analysis.

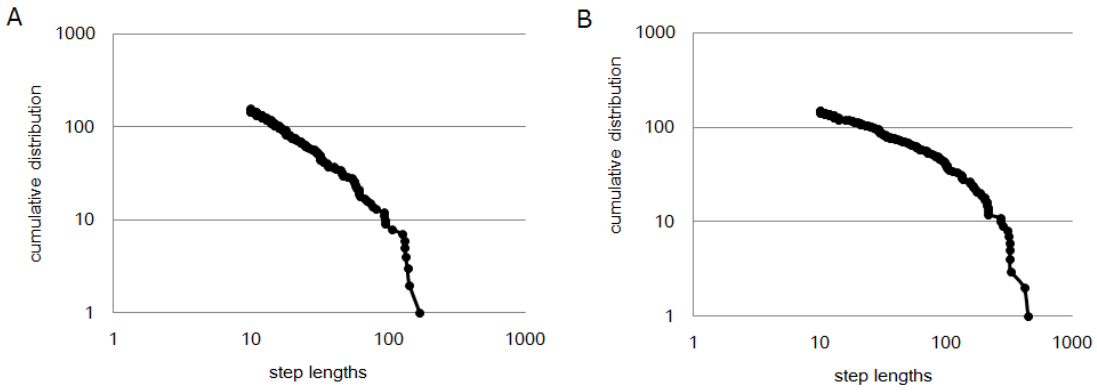

Figure S1. Log-log plots of simulation step lengths and cumulative distribution with respect to detection values different from the default value (2.00 radii). A. 1.00 radii. B. 3.00 radii.

Bibliography

1 Boyer, D.S. & Larralde, H. 2005 Looking for the Right Thing at the Right Place: Phase Transition in an Agent Model with Heterogeneous Spatial Resources. *Complexity* 10, 52–55.

2 Santos M. C., Boyer, D.S, Miramontes, O., Viswanathan, G. M., Raposo, E. P., Mateos, J. L. and Luz, M. G. E. 2007 Origin of power-law distributions in deterministic walks: The influence of landscape geometry. *Phys. Rev. E*.75 (061114), 1-6.

3 Kareiva, R.M. & Shigesada, N. 1983 Analyzing Insect Movement as a Correlated Random Walk. *Oecologia (Berlin)* 56, 234-238.

4 Viswanathan, G. M., Afanasyev, V., Buldyrev, S.V., Havlin, S., Luz, M. G. E., Raposo, E.P. and Stanley, H.E. 2001 Statistical Physics of Random Searches. *Braz J. Phys.* 31(1), 102-108.

5 Bartumeus, F., Luz, M. G. E., Viswanathan, G.M. & Catalan, J. 2005 Animal Search Strategies: A Quantitative Random-Walk Analysis. *Ecology* 86(11), 3078-3087

6 Bartumeus, F., Catalan, J., Viswanathan, G.M., Raposo, E.P. & Luz., M.G.E. 2008 The influence of turning angles on the success of non-oriented animal searches. *J. Theor. Biol.* 252, 43-55

7 Bartumeus, F. & Levin, S.A. 2008 Fractal reorientation clocks: Linking animal behavior to statistical patterns of search. *Proc. Natl Acad. Sci. USA.* 105(49), 19072–19077

8 Viswanathan, G.M., Afanasyev, V., Buldyrev, S.V., Murphy, E.J., Prince, P.A. & Stanley, H.E. 1996 Lévy flight search patterns of wandering albatrosses. *Nature* 381, 413 - 415

9 Bartumeus, F., Catalan, J., Fulco, U.L., Lyra, M.L. & Viswanathan, G.M. 2002 Optimizing the Encounter Rate in Biological Interactions: Lévy versus Brownian Strategies. *Phys. Rev. Lett* 88(9), 097901-1-097901-4

10 Faustino, C.L., Silva, L.R., Luz, M.F.E., Raposo, E.P. & Viswanathan G.M. 2007 Search dynamics at the edge of extinction: Anomalous diffusion as a critical survival state. *J. Exp. Front. Phys.* 77(30002), 1-6

11 Humphries, N.E., Weimerskirch, H., Queiroz, N., Southall, E.J., & Sims, D.W. 2012 Foraging s uccess of biological Lévy flights recorded in situ. *Proc. Natl Acad. Sci. USA.* 109(19), 7169-7174

12 Sueur, C., Briard, L. & Petit, O. 2011 A Non- Lévy Random Walk in Chacma Baboons: What Does It Mean? *PLOS ONE* 6(10), 1-8

13 Sims, D.W., Humphries, N.E., Bradford, R.W. & Bruce, B.D. 2012 Lévy flight and Brownian search patterns of a free-ranging predator reflect different prey field characteristics. *J. Anim. Ecol.* 81, 432–442

14 López-López, P., Benavent-Corai, L., García-Ripollés, C. & Urios, V. 2013 Scavengers on the Move: Behavioural Changes in Foraging Search Patterns during the Annual Cycle. *PLOS ONE*

8(1), e54352 (doi: 10.1371/journal.pone.0054352)

15 Viswanathan, G.M., Raposo, E.P., Luz, M.G.E. 2008 Lévy flights and superdiffusion in the context of biological encounters and random searches. *Phys. Life Rev.* 5, 133-150

16 Fronhofer, E.A., Hovestadt T. & Poethke, H.J. 2012 From random walks to informed movement. *Oikos* 000, 001–010

17 Viswanathan, G.M., Raposo, E.P., Bartumeus, F., Catalan, J. & Luz, M.G.E. 2005 Necessary criterion for distinguishing true superdiffusion from correlated random walk processes. *Phys. Rev. E* 72(011111), 1-6

18 Edwards, A.M., Phillips, R.A., Watkins, N.W., Freeman, M.P., Murphy, E.J., Afanasyev, V., Buldyrev, S.V., Luz, M.G.E., Raposo, E.P. & Stanley, H.E. 2007 Revisiting Lévy flight search patterns of wandering albatrosses, bumblebees and deer. *Nature* 449(25), 1044-1049

19 Schultheiss, P., Cheng, K. 2011 Finding the nest: inbound searching behaviour in the Australian desert ant, Melophorus bagoti. *Anim. Behav.* 81, 1031-1038

20 Lamine, K., Lambin, M. & Alauzet, C. 2005 Effect of starvation on the searching path of the predatory bug Deraeocoris lutescens. *Bio. Control.* 50, 717–727

21 Skoglund, H. & Barlaup, B.T. 2006 Feeding pattern and diet of first feeding brown trout fry under natural conditions. *Journal. Fish Biol.* 68, 507–521

22 Schultheiss, P., Wystrach, A., Legge, E.L.G. & Cheng, K. 2013 Information content of visual scenes influences systematic search of desert ants. *J. Exp. Biol*. 216, 742-749

23 Humphries, N.E., Queiroz, N., Dyer, J.R.M., Pade, N.G., Musy, M.K., Schaefer, K.M., Fuller, D.W., Brunnschweiler, J.M., Doyle, T.K., Houghton, J.D.R., Hays, G.C., Jones, C.S.,Noble, L.R., Wearmouth, V.J., Southall, E.J. & Sims, D.W. Environmental context explains Lévy and Brownian movement patterns of marine predators. 2010 *Nature* 465, 1066–1069

24 Detrain, C. & Deneubourg, J.L. 2006 Self-organized structures in a superorganism: do ants “behave” like molecules? *Phys. Life Rev.* 3, 162–187

25 Zeil, J. 2012 Visual homing: an insect perspective. Curr. Opin. Neurobiol. 7, 1-22

26 Cheng, K. 2012 How to navigate without maps: The power of taxon-like navigation in ants. Comp Cogn & Behav Rev. 7, 1-22

27 Sakiyama, T. and Gunji, Y.P. 2013 Emergence of an optimal search strategy from simple random walk. *J. R. Soc. Interface* 10(86), 1-6

28 Viswanathan, G.M., Buldyrev, S.V., Havlin, S., Luz, M. G. E., Raposo, E.P. and Stanley, H.E. Optimizing the success of random searches. 1999 *Nature* 401, 911-914

29 Humphries, N.E., Weimerskirch, H., Sims, D.W. 2013 A new approach to objective identification of turns and steps in organism movement data relevant to random walk modelling. *Methods in Ecology and Evolution*, 4(10), 930-938, doi:10.1111/2024-210X.12096

30 Reynolds, A.M. 2010 Bridging the gulf between correlated random walks and Le´vy walks:

autocorrelation as a source of Lévy walk movement patterns. *R. Soc. Interface* 7, 1753-1758

31 Reynolds, A.M. 2012 Olfactory search behaviour in the wandering albatross is predicted to give rise to Lévy flight movement patterns. *Anim. Behav* 83, 1225-1229

32 Reynolds, A.M. 2013 Effective leadership in animal groups when no individual has pertinent information about resource locations: How interactions between leaders and followers can result in Lévy walk movement patterns. *A Lett. J. Exp. Front. Phys* 102, 18001

33 Sims, D.W. et al. 2008 Scaling laws of marine predator search behaviour. ‚*Nature*. 451, 1098-1102.

34 de Jager, M.,Weissing, F. J., Herman, P.M., Nolet, B. A. & van de Koppel, J. 2011 Le´vy walks evolve through interaction between movement and environmental complexity. ‚*Science*. 332, 1551–1553.

35 Harris, T. H. et al. 2012 Generalized Lévy walks and the role of chemokines in migration of effector CD8+ T cells. ‚*Nature*. 486, 545-548.

36 Raichlen, D.A. et al. 2013 Evidence of Lévy walk foraging patterns in human hunter–gatherers. ‚*Proc. Natl Acad. Sci. USA*. 111(2), 728–733, doi: 10.1073/pnas.131861611.

37 Weber, E.H. Tastsinn und Gemeingefühl. 1846 In: Wagner R (ed) Handwörterbuch der Physiologie, vol III. Vieweg, Braunschweig, 481–588.

38 Fechner, G.T. 1860 Elemente der Psychophysik. Breitkopf und Härtel, Leipzig.

39 Gabaix, X. 1999 Zipf's law for cities: an explanation. ‚*Q J Econ*. 114, 739–767.

40 Reynolds, A.M., Schultheiss, P. & Cheng, K. 2013 Are Lévy flight patterns derived from the Weber–Fechner law in distance estimation? ‚*Behav Ecol Sociobiol*. 67(8), 1219-1226, DOI 10.1007/s00265-013-1549-y.

41 Sakiyama, T. & Gunji, Y. P. 2014 The relationship between randomness and power-law distributed move lengths in random walk algorithms. ‚*Physica A*. 402, 76–83.

42 Reynolds, A.M., Leprétre, L. & Bohan, D.A. 2013 Movement patterns of Tenebrio beetles demonstrate empirically that correlated-random-walks have similitude with a Lévy walk. ‚*Scientific Reports*. 3 (3158), 1-8.

43 Kearney, M. J. & Majumdar, S. N. 2005 On the area under a continuous time Brownian motion till its first-passagetime. ‚*J. Phys. A*. 38, 4097–4104. (doi:10.1088/0305-4470/38/19/004).

44 Johnson, D. S., London, J. M., Lea, M. A. & Durban, J. W. 2008 The continuous-time correlated random walk model for animal telemetry data. ‚*Ecology*. 89, 1208–1215 (doi:10.1890/07-1032.1).

45 Mlot, N.J., Tovey, C.A. & Hu, D.L. 2011 Fire ants self-assemble into waterproof rafts to survive floods. ‚*Proc. Natl Acad. Sci. USA*. 108, 7669-7673.

46 Jürgens, R. & Becker, W. 2006 Perception of angular displacement without landmarks: evidence for Bayesian fusion of vestibular, optokinetic, podokinesthetic, and cognitive

information. *Exp. Brain. Res.* 174, 528 –543.

47 Stocker, A. A. & Simoncelli, E. P. 2006 Noise characteristics and prior expectations in human visual speed perception. *Nat. Neurosci.* 9, 578–585.

48 Jazayeri, M. & Shadlen, M. N. 2010 Temporal context calibrates interval timing. *Nat. Neurosci.* 13, 1020–1026.

49 Petzschner, F.H. & Glasauer, S. 2011 Iterative Bayesian estimation as an explanation for regression and range effects – a study on human path integration. *J. Neurosci.* 31(47), 17220-9.

50 Dehaene, S., Izard, V., Spelke, E. & Pica, P. 2008 Log or linear? Distinct intuitions of the number scale in Western and Amazonian indigene cultures. *Science.* 320, 1217–1220.

51 Durgin, F.H., Akagi, M., Gallistel, C. R. & Haiken, W. 2009 The precision of locomotor odometry in humans. *Exp. Brain. Res.* 193, 429–436.

52 Mailleux A-C, Deneubourg J-L, Detrain C 2000 How do ants assess food volume? *Animal Behaviour*, 59, 1061–1069.

53 Jeanson R, Deneubourg J-L, Theraulaz G 2004 Discrete dragline attachment induces aggregation in spiderlings of a solitary species. *Animal Behaviour* 67, 531–537.

54 Wehner R, Boyer M, Loertscher F, Sommer S, Menzi U 2006 Ant Navigation: One-Way Routes Rather Than Maps. *Current Biology,* 16: 75–79.

55 Sakiyama T, Gunji Y-P 2013 The Müller-Lyer Illusion in Ant Foraging. *PLOS ONE* (8)12: e81714

56 Palyulina V-V, Chechkin A-V, Metzler R 2014 Lévy flights do not always optimize random blind search for sparse targets. *Proc. Natl Acad. Sci. USA*. 111(8), 2931–2936, doi: 10.1073/pnas.1320424111

57 Schultheiss P, Cheng K 2013 Finding food: outbound searching behavior in the Australian desert ant Melophoru sbagoti. *Behavioral Ecology* 24, 128–135.

58 Narendra A, Cheng K, Sulikowski D, Wehner R 2008 Search strategies of ants in landmark-rich habitats. *Journal of Comparative Physiology A*, 194, 929-938.

59 Reynolds A-M, Schultheiss P, Cheng K 2014 Does the Australian desert ant Melophorus bagoti approximate a Lévy search by an intrinsic bi-modal walk? *Journal of Theoretical Biology* 340, 17–22

60 Reynolds A-M 2014 Mussels realize Weierstrassian Lévy walks as composite correlated random walks. *Scientific Reports* 4(4409), 1-5.

61 Jansen VAA, Mashanova A, Petrovskii S. 2012 Comment on ‘‘Le´vy walks evolve through interaction between movement and environmental complexity.” *Science* 335, 918

62 de Jager M, Weissing F-J, Herman P-M, Nolet B-A, van de Koppel J 2012 Response to Comment on ‘‘Le´vy walks evolve through interaction between movement and environmental complexity’’ *Science* 335, 918.

63 Collett M, Collett TS, Bisch S, Wehner R. 1998 Local and global vectors in desert ant. *Nature* 394, 269-272.

64 Graham P. and Cheng K. 2009. Ants use the panoramic skyline as a visual cue during navigation. *Curr. Biol*. 19, 935-937

65 Graham, P., Philippides, A., Baddeley, B. 2010 Animal Cognition: Multi-modal Interactions in Ant Learning. *Curr Biol*. 20, 639-640

66 Baddeley B, Graham P, Philippides A and Husbands P. 2012 A Model of Ant Route Navigation Driven by Scene Familiarity. P*LoS Comput Biol* 8(1): e1002336.

67 Fujita, K. 2001 Perceptual completion in rhesus monkeys (Macaca mulatta) and pigeons (Columba livia), *Percep & Psychophy*, 63(1), 115-125.

68 Hopkins, W.D. & Washburn, D.A. 2002 Matching visual stimuli on the basis of global and local features by chimpanzees (Pan troglodytes) and rhesus monkeys (Macaca mulatta), *Anim Cogn*, 5, 27-32.

69 Nagasaka, T., Hori, K. & Osada, Y. 2005 Perceptual grouping in pigeons. *Perception*. 34(5), 625-632.

70 Vallortigara, G., Snyder, A., Kaplan, G., Bateson, P., Clayton, N. S. & Rogers, L.J. 2008 Are Animals Autistic Savants? *PLOS Biol*, 6(2), 0208-0214.

71 Matsukawa, A., Inoue, S. & Jitsumorivol, M. 2004 Pigeon's recognition of cartoons: effects of fragmentation, scrambling, and deletion of elements, *Behav Proc*, 65, 25-34.

72 Kanizsa, G. 1976 Subjective contours, *Sci Am*, 234, 48-52.

73 Kanizsa, G. 1979 Organization in Vision: Essays on Gestalt Perception, *Praeger Publishers,* ISBN 0275903737

74 Wang, L., Weng, X & He, S. 2012 Perceptual Grouping without Awareness: Superiority of Kanizsa Triangle in Breaking Interocular Suppression, *PLOS ONE*, 7(6), 1-6.

75 Deneubourg J.L., Pasteels, J.M. & Verhaeghe, J.C. 1983 Probabilistic Behaviour in Ants: A Strategy of Errors? *J. theor. Biol*. 105, 259-271.

76 Mailleux, A.C., Deneubourg, J.L. & Detrain, C. 2009 Food transport in ants: Do Lasius niger foragers maximize their individual load? *C R Biol*, 332(5), 500-6

77 Tao, T., Nakagawa, H., Yamasaki, M. & Nishimori, H. 2004 Flexible Foraging of Ants under Unsteadily Varying Environment. *Journal of the Physical Society of Japan*, 73(8), 2333–2341.

78 Beckers R., Deneubourg J.L. and Goss S. 1992. Trail laying behaviour during food recruitment in the ant Lasius niger (L). *Insect. Soc*. 39, 59-72

79 Beckers R., Deneubourg J.L. and Goss S. 1992. Trails and U-turns in the Selection of a Path by the Ant Lasius niger, *J. theor. Biol*. 159, 397-415

80 Ebert, J.P. & Wegner, D.M. 2010 Time warp: Authorship shapes the perceived timing of actions and events. *Consciousness and Cognition* 19, 481–489

81 Moore, J.M., Lagnado, D., Deal, D.C. & Haggard, P. 2009 Feelings of control: Contingency determines experience of action. *Cognition* 110, 279–283

82 Tani, I., Yamachiyo, M., Shirakawa, T. & Gunji, Y.P. 2014 Kanizsa illusory contours appearing in the plasmodium pattern of Physarum polycephalum. *Front. Cell. Infect. Microbiol* 4(10), 1-11